Nature and Science of Sleep

Elevate Series

Open Access Full Text Article

ORIGINAL RESEARCH

Exosomes from IH- Induced bEnd3 Cells Promote OSA Cognitive Impairment via miR-20a-5p/MFN2 Mediated Pyroptosis of HT22 Cells

Zhifeng Chen[1–4], Yulin Shang[5], Yanru Ou[1–4], Li Zhou[1–4], Ting Liu[1–4], Subo Gong[6], Xudong Xiang[7], Yating Peng[1–4], Ruoyun Ouyang[1–4]

[1]Department of Pulmonary and Critical Care Medicine, The Second Xiangya Hospital, Central South University, Changsha, Hunan, 410011, People's Republic of China; [2]Research Unit of Respiratory Disease, Central South University, Changsha, Hunan, 410011, People's Republic of China; [3]Clinical Medical Research Center for Pulmonary and Critical Care Medicine in Hunan Province, Changsha, Hunan, 410011, People's Republic of China; [4]Diagnosis and Treatment Center of Respiratory Disease, Central South University, Changsha, Hunan, 410011, People's Republic of China; [5]Ophthalmology and Otorhinolaryngology, Zigui Country Hospital of Traditional Chinese Medicine, Yichang, Hubei, 443600, People's Republic of China; [6]Department of Geriatrics, The Second Xiangya Hospital, Central South University, Changsha, Hunan, 410011, People's Republic of China; [7]Department of Emergency, The Second Xiangya Hospital, Central South University, Changsha, Hunan, 410011, People's Republic of China

Correspondence: Yating Peng; Ruoyun Ouyang, Department of Pulmonary and Critical Care Medicine, The Second Xiangya Hospital, Central South University 139 Middle Renmin Road, Changsha, Hunan, 410011, People's Republic of China, Email pengyating2011@csu.edu.cn; ouyangruoyun@csu.edu.cn

Background: OSA can cause cognitive impairment (CI). The aim of this study was to investigate whether miR-20a-5p in exosomes derived from bEnd3 cells with IH mediates intercellular crosstalk and induces CI through hippocampal neuronal cell pyroptosis.

Materials and Methods: BEnd3-derived exosomes were isolated from the normal oxygen control group (NC-EXOS) and IH group (IH-EXOS). In vitro, exosomes were cocultured with HT22 cells. Meanwhile, in vivo, exosomes were injected into mice via the caudal vein. The spatial memory ability of mice was tested by MWM method to evaluate the effect of exosomes on the cognitive function of mice. Adults diagnosed with OSA underwent the MoCA and ESS tests to assess cognitive function and daytime sleepiness. Spearman's rank correlation analysis was used to evaluate the correlation between miR-20a-5p and candidate proteins and clinical parameters. Transfection using small interfering RNAs, miRNA mimics, and plasmids to evaluate the role of miR-20a-5p and its target genes. Dual luciferase reporter gene assay was used to confirm the binding of miR-20a-5p to its target gene.

Results: IH could cause pyroptosis and inflammation in bEnd3 cells, and promote the expression of miR-20a-5p. Isolated IH-EXOS induced increased pyroptosis and activation of inflammatory response in vitro and in vivo, accompanied by increased expression of miR-20a-5p. In addition, IH-EXOS led to decreased learning and memory ability in mice. Interestingly, AHI was higher and MoCA scores were lower in severe OSA compared to healthy comparisons. In addition, miR-20a-5p and GSDMD were positively correlated with AHI but negatively correlated with MoCA in severe OSA. IH-induced exosomes were rich in miR-20a-5p, and these exosomes were found to deliver miR-20a-5p to HT22 cells, playing a key role in the induction of OSA-CI by directly targeting MFN2.

Conclusion: Exosome miR-20a-5p from IH-stimulated bEnd3 cells can promote OSA-CI by increasing HT22 cells pyroptosis through its target MFN2.

Keywords: exosome, OSA, cognitive impairment, miR-20a-5p, MFN2, GSDMD

Introduction

Obstructive sleep apnea (OSA) is a chronic respiratory disorder that occurs more often in middle-aged and older adults and is characterized by intermittent hypoxia (IH) during sleep due to recurrent upper airway obstruction.[1] Studies have found that OSA is a risk factor for promoting cognitive impairment (CI), which may be related to IH induced inflammatory response activation and endothelial cell dysfunction.[2,3] Current research has shown that the hippocampus is the most morphologically altered area of the brain in OSA patients, which may be related to the damage to the hippocampus caused by hypoxia.[4] Endothelial cells line the walls of brain capillaries and are the main components of the blood-brain barrier (BBB).[5] Some studies have found that the increase of cerebrospinal fluid and abnormal expression of

Received: 6 August 2024
Accepted: 7 December 2024
Published: 17 December 2024

aquaporin in mice exposed to IH indicate that the destruction of BBB leads to an increase in permeability, which may be the basis for the occurrence of OSA-associated CI (OSA-CI).[6]

Pyroptosis is a pro-inflammatory programmed cell death mediated by Gasdermin D (GSDMD), a pore formation efficant induced by classical Caspase-1, which can also induce the release of interleukin (IL-1β), IL-18, and activate the inflammatory response, resulting in physiological imbalance in the body.[7,8] In a mouse model induced to Alzheimer's disease (AD), elevated levels of GSDMD were found, as well as reduced cognitive function in the mice, but when pyroptosis was inhibited, the memory and behavior of the mice improved.[9] Increased expression of pyroptosis and inflammatory factors has been found in hypoxia-induced OSA models, but whether they are related to OSA-CI remains unclear.[10]

Exosomes can be secreted by a variety of cells, exist in urine, blood, and other places, with a diameter between 30 and 150 nm, is a subclass of extracellular vesicles, and plays a role in transmitting biological signals between cells.[11] In addition to proteins, exosomes have also been identified to contain various nucleic acids, including microRNAs (miRNAs).[12] Exosomal miRNAs are a class of small non-coding RNAs, which regulate gene expression by binding to the 3'-non-translation region of target mRNA, thus playing a role as communication carriers between cells.[13] Plasma exosomes acquired prior to OSA treatment cause dysfunction of naive endothelial cells, and these changes are mediated by selective components of exosomal miRNAs.[14] Khalyfa et al found that OSA plasma-derived exosomes were co-cultured with endothelial cells, and found that they could cause the decrease of BBB impedance and abnormal expression of Zonula occludens-1, thus disrupting the integrity of BBB, which is a risk factor for cognitive deficits.[15] It was found that miR-20a-5p has a regulatory effect on lipopolysaccharides-induced pyroptosis, and the plasma-derived exosome miR-20a-5p is associated with the occurrence of AD.[16,17] We previously found that the plasma-derived exosomes of OSA increased the pyroptosis of hippocampal neurons and impaired the spatial memory learning ability of mice. Through RNA sequencing, unique miRNAs profiles, including miR-20a-5p, were identified in the plasma-derived exosomes of severe OSA.[18] It has not yet been determined whether IH-induced exosomes, especially miR-20a-5p, promote OSA cognitive decline. The underlying mechanism of OSA-CI remains unclear at present, highlighting the critical importance of investigating its potential mechanisms to inform the development of effective treatment strategies.

In this study, we aimed to identify the potential role of IH-induced exosomes in OSA-associated cognitive deficits. Our study showed that IH-induced exosomes accelerate CI and activate inflammatory responses through pyroptosis.

Materials and Methods

IH Cell Model

Endothelial cells are the primary constituent cells of BBB. Given that IH can cause damage to the BBB, we established an in vitro model of OSA by subjecting mouse brain microvascular endothelial (bEnd3) cells to IH according to a previously reported protocol.[19] BEnd3 cells were acquired from Cellverse Bioscience Technology Co., Ltd (Shanghai, China). The cells were cultured at 37°C, 5% CO2, where cell media contained 10% exosome-depleted fetal bovine serum (FBS), in the IH exposure group (IH), where 1% O2 was 5 minutes (min) and 21% O2 was 10 min, while the control group was exposed to 21% O2 in normoxic air (NA) for 18 hours (h). The gas flows were regulated by a computerized solenoid valve. O2 levels were monitored through electrodes embedded in the tissue culture medium, and ambient O2 levels were simultaneously monitored using an O2/CO2/N2 analyzer (Hariolab, Zhejiang, China).

Exosome Isolation

Exosomes are isolated from bEnd3 cell supernatants, and these methods have been described previously.[20] Briefly, the isolated cell supernatant underwent an initial centrifugation (2000×g for 10 min) to discard cell debris, then centrifugation at 10,000×g for 30 min and ultracentrifugation at 100,000×g (Optima L-100XP, Beckman Coulter, USA) for 120 min. Exosomes were washed once with 1xPBS and centrifuged again at 100,000×g for 120 min. All steps were performed at 4°C. Exosomes isolated from NA and IH were defined as NC-EXOS and IH-EXOS, respectively. The concentration of concentrated exosomes was determined by bicinchoninic acid assay (Beyotime, Shanghai, China) and the exosomes were stored at −80°C or for subsequent experiments. Exosome specific markers such as CD9 and CD63 (Proteintech, Wuhan, China) were used for identification by Western blot.

Transmission Electron Microscope and Size Distribution

Exosome morphology was observed by transmission electron microscopy (TEM), and imaging was performed under 80 kV TEM (HT7700 TEM). The nanoparticle tracking analysis (NTA) was performed using the ZetaView PMX 110 instrument (Particle Metrix, Germany) to determine vesicle size. Created a particle size distribution plot where the X-axis represents the distribution of the estimated particle size (nm), and the Y-axis estimates the concentration (particles/mL).

Exosome Labelling and Cellular Uptake

The concentrated exosomes were tagged with the membrane labeling dye PKH67-Green (Sigma-Aldrich, USA) following the instructions, then washed and resuspended in serum-free medium. Next, hippocampal neurons (HT22) cells were then co-cultured with PKH67-labeled exosomes for 24h and imaged with inverted fluorescence microscopy (Olympus IX73). HT22 cells were acquired from Cellverse Bioscience Technology Co., Ltd (Shanghai, China).

In vivo Imaging of Fluorescently Labelled Exosomes

PKH67-labeled exosomes (100 μg/mouse) were injected into male mice through the tail vein. After 48h, mouse hippocampal tissue was imaged in vitro to evaluate the distribution of PKH67-labeled exosomes in vivo.

Exosomes Coculture

GW4869 can block exosome secretion. GW4869 (Sigma-Aldrich, USA, 10 μM) was added to bEnd3 cells at IH and exosomes were isolated (IH-EXOS + GW4869).[21] IH can impair hippocampal function. To evaluate the effects of IH-induced exosomes on the hippocampus, we treated HT22 cells with NC-EXOS, IH-EXOS, IH-EXOS + GW4869 (10 μg/μL, 100 μg/well) or equivalent PBS (normal control) for 24h in growth medium containing 10% exosome-depleted FBS.[22]

Exosome Intervention in vivo

Male C57BL/6 mice (8 weeks of age, 18–20g, n=15) were provided by the Animal Center of Central South University and raised under specific pathogen free conditions. The animal experiment procedure was approved by the Animal Care and Use Committee of Central South University and was carried out in accordance with the guiding principles of the Laboratory Animal Department of Central South University and the State Science and Technology Commission on the care and use of laboratory animals. Fifteen mice were randomly divided into non-exosome intervention PBS group (NC, n=5), normoxic air-derived exosome intervention group (NC-EXOS, n=5) and IH-induced exosome intervention group (IH-EXOS, n=5). On day 0, NC-EXOS and IH-EXOS (10 μg/μL, 100 μg/mouse) were injected via the tail vein, and the NC group was given an equal dose of 1xPBS in the same manner. After that, the mice were given either exosomes or PBS every 3 days for 4 weeks.[22]

Morris Water Maze (MWM) Test

The mice's spatial learning and memory abilities were assessed using the Morris Water Maze (MWM) test as previously described.[23] Mice were tested for MWM during the last 6 days of exosome intervention. Briefly, the mice were trained in spatial learning two times a day for five days. The escape latency was defined as the time it took the mice to find a hidden platform underwater. The retention test was conducted the day after the last acquisition session. The percentage of time the mice traveled in the target quadrant and the number of times they crossed the platform were recorded on day 6.

Histopathology and Immunohistochemistry

After the MWM test, mice were anesthetized with isoflurane and then killed (n=5/group). Half hemisphere (left) was removed, fixed with 4% paraformaldehyde, then embedded with paraffin wax, sectionalized (5μm), and stained with hematoxylin and eosin (H&E), Nissl staining, and immunohistochemistry [GSDMD antibody, Caspase-1 antibody (Proteintech, Wuhan, China)]. The right hemisphere hippocampal tissue was preserved at −80°C for follow-up experiments.

Subjects

The Ethics Committee of the Second Xiangya Hospital of Central South University approved this study (Ethical Code: LYF2023059), all subjects signed an informed consent form and all experiments were conducted in accordance with the Declaration of Helsinki. Initially, we included 108 OSA patients registered at the inpatient Department of Respiratory and Critical Care Medicine, Second Xiangya Hospital, Central South University between June 2022 and May 2023. Cessation of airflow ≥10s was defined as apnea, and hypoxia was defined as a decrease of airflow of at least 30% ≥10s accompanied by a decrease in blood oxygen saturation.[24] The apnea hypopnea Index (AHI) was used to define the severity of OSA, with AHI ≥30 events/h defined as severe OSA.[25] The following inclusion criteria were used for patients with severe OSA: (a) according to the American Academy of Sleep Medicine Clinical Practice Guideline, OSA was diagnosed by polysomnography (PSG) with an AHI ≥5 events/h;[26] (b) the symptoms of OSA attacks were frequent, including snoring, daytime sleepiness, nighttime awakenings, and AHI ≥30 events/h; (c) at least 18 years of age. And the following patients were excluded: (a) use of hypnotic drugs or major depression; (b) serious infection, trauma, tumor, cardiopulmonary disease or neurodegenerative diseases; (c) other sleep disorders, such as insomnia or narcolepsy or restless leg syndrome; (d) CI without OSA, stroke, or pregnant women. Health comparisons (HCs) had AHI <5 events/h and no history of CI. A detailed description of the flow diagram for recruiting voluntary patients can be found in Figure 1.

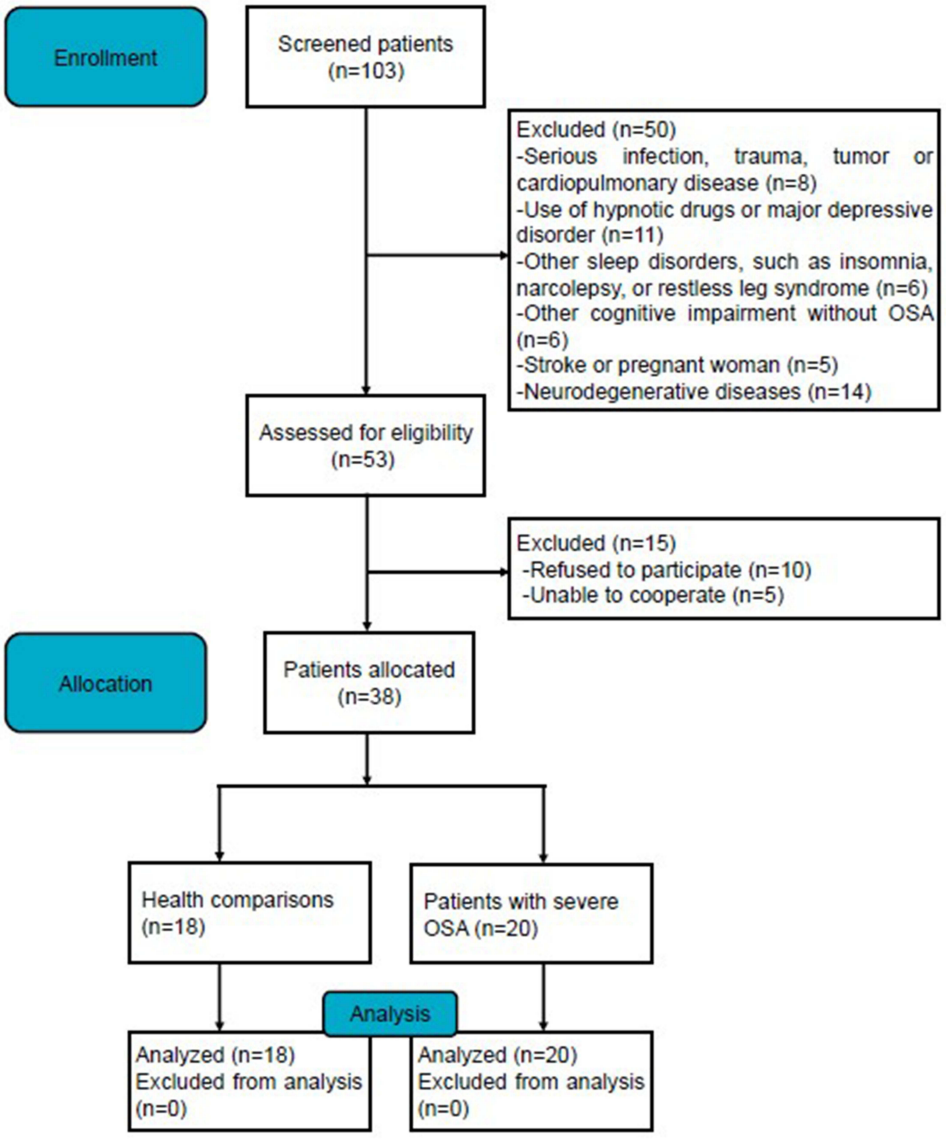

Figure 1 Flow diagram of the study.

Data and Blood Sample Collection

Gender, age, education, body mass index (BMI), smoking status, PSG monitoring, Epworth Sleepiness Scale (ESS) and Beijing Montreal Cognitive Assessment Scale (MoCA) were recorded for each volunteer after signing a written informed consent form. An ESS score ≥10 was defined as associated with excessive daytime sleepiness and a MoCA score <26 was defined as associated with cognitive dysfunction.[27,28] Whole blood was collected from each subject using EDTA tubes before treatment and at least 8h fasting, and peripheral blood mononuclear cells (PBMCs) were isolated by density gradient centrifugation.[29]

Cell Transfection

miR-20a-5p inhibitor and Cy3-labelled mimics (inhibitor miR-20a-5p, mimics miR-20a-5p), as well as corresponding negative controls (inhibitor-NC miR-20a-5p, mimics-NC miR-20a-5p), as well as small interfering RNA targeting mitofusin 2 (siR MFN2) and negative control (siR-NC MFN2) were purchased from RuiBo (Guangzhou, China). The MFN2 interfering sequence was 5'-CGGTTCGACTCATCATGGA-3'. The overexpression plasmid targeting MFN2 (OE MFN2), and negative control (OE-NC MFN2) were acquired from HonorGene (Hunan, China). The cells were transfected with miR-20a-5p inhibitor and mimics, and small interfering RNA and plasmid for 48h using Lipofectamine 3000 (Invitrogen) according to the manufacturer's protocol. After 2 days, the cells were cultured with IH-EXOS (10 μg/μL, 100 μg/well) or equal-volume PBS in exosome-depleted medium for 24h.

Western Blot

The right hippocampal tissue and cells were dissolved in radioimmunoprecipitation buffer. Protein samples of 25 μg were transferred to the membrane by 1–1.5h sodium dodecyl sulphate-polyacrylamide gel electrophoresis. Appropriately diluted CD9, CD63, GSDMD, Caspase-1 and GAPDH (Proteintech, Wuhan, China) antibodies were then incubated at 4°C overnight. The Image was obtained using a chemiluminescent gel imaging system and the band intensity was measured using Image J software. The relative protein expression level was calculated by the ratio of target band gray value to GAPDH gray value and normalized.

Quantitative Real-Time PCR

Total RNA from hippocampal tissues, bEnd3 and HT22 cells, and PBMCs was extracted with TRIzol reagent (Invitrogen) according to the instructions. Exosomal RNA was isolated using the miRNeasy Mini Kit (Qiagen, Germany). Using PrimeScript RT reverse transcriptase kit (Takara, Japan) to synthesize cDNA. Quantitative real-time fluorescent quantitative PCR (qRT-PCR) was performed using the SYBR Premix Ex Taq kit (Takara, Japan). U6, mouse β-actin and human GAPDH were used as internal parameters. According to the cycle threshold (Ct) value of the samples, the gene expression was calculated by $2^{-\Delta\Delta Ct}$ method. The target gene primers were manufactured by Sangon Biotechnology (Shanghai, China). Stem-loop primer for miR-20a-5p: 5'-GTCGTATCCAGTGCAGGGTCCGAGGTATTCGCACTGGA-3'. The primer sequences can be found in Table 1.

Enzyme-Linked Immunosorbent Assay

The levels of IL-1β, IL-6, IL-18 and TNF-α in mouse serum and cell supernatant were measured using enzyme-linked immunosorbent assay (ELISA) kits. The mouse IL-1β ELISA Kit (KE10003, Proteintech, China), mouse IL-6 ELISA Kit (KE10007, Proteintech, China), mouse IL-18 ELISA Kit (JL20253, Jianglai, China), and mouse TNF-α ELISA Kit (KE10002, Proteintech, China) were utilized for this purpose. All experimental steps were carried out in accordance with their respective guidelines.

Dual Luciferase Reporter Assay

Both double luciferase reporter vector plasmids carrying MFN2 3'UTR wild type (WT) or mutant type (MUT) and miR-20a-5p mimics were co-transfected into HEK293T cells with Lipofectamine 3000 (Invitrogen). After 48h incubation,

Table 1 Primer Sequences of the Study

Gene Symbol	Forward	Reverse
miR-20a-5p	5′-CGCGGCCTAAAGTGCTTATAGTG-3′	5′-ATCCAGTGCAGGGTCCGAGG-3′
U6	5′-CTCGCTTCGGCAGCACA-3′	5′-AACGCTTCACGAATTTGCGT-3′
Human GSDMD	5′-GCCTCCACAACTTCCTGACAGATG-3′	5′-GGTCTCCACCTCTGCCCGTAG-3′
Human Caspase-1	5′-TCCTCAGGCTCAGAAGGGAATGTC-3′	5′-GTGCGGCTTGACTTGTCCATTATTG-3′
Human MFN2	5′-AGCAGATTACGGAGGAAGTGGAGAG-3′	5′-GAGGACTACTGGAGAAGGGTGGAAG-3′
Human IL-1β	5′-GGACAGGATATGGAGCAACAAGTGG-3′	5′-TCATCTTTCAACACGCAGGACAGG-3′
Human IL-6	5′-GCCTTCGGTCCAGTTGCCTTC-3′	5′-GTTCTGAAGAGGTGAGTGGCTGTC-3′
Human IL-18	5′-GCATCAACTTTGTGGCAATG-3′	5′-GCCGATTTCCTTGGTCAAT-3′
Human TNF-α	5′-CCTCATCTACTCCCAGGTCCTCTTC-3′	5′-TCTGGTAGGAGACGGCGATGC-3′
Human GAPDH	5′-CAGGAGGCATTGCTGATGAT-3′	5′-GAAGGCTGGGGCTCATTT-3′
Mouse GSDMD	5′-CGATGGGAACATTCAGGGCAGAG-3′	5′-ACACATTCATGGAGGCACTGGAAC-3′
Mouse Caspase-1	5′-ATACAACCACTCGTACACGTCTTGC-3′	5′-TCCTCCAGCAGCAACTTCATTTCTC-3′
Mouse MFN2	5′-GCATTCTTGTGGTCGGAGGAGTG-3′	5′-TGGTCCAGGTCAGTCGCTCATAG-3′
Mouse *β*-actin	5′-GTGCTATGTTGCTCTAGACTTCG-3′	5′-ATGCCACAGGATTCCATACC-3′

luciferase activity was measured using the dual-luciferase assay system (Promega). The normalized renilla luciferase activity was compared among all groups.

Statistics Analysis

All experiment in this study was carried out at least 3 times. For statistical analysis, SPSS 26.0 software (IBM Corp). was used, and images were generated by GraphPad Prism 9.0.0 software (GraphPad Software Inc). Continuous variables were described as mean and standard deviation (M ± SD), and categorical variables were expressed as the number (percentage). The Student's *t*-test and chi-square test or Fisher's precision test were used to determine statistical differences between the two groups, as well as one or two-way analysis of variance (ANOVA) followed by Bonferroni multiple comparison tests to determine statistical differences between the three groups. Spearman's rank correlation test was used for correlation among parameters. A P-value<0.05 was considered statistically significant.

Results

IH Promotes Pyroptosis and Inflammation of bEnd3 Cells

Endothelial cells are an important part of BBB, and studies have found that OSA can cause BBB dysfunction.[6] Endothelial pyroptosis is an important biological behavior of BBB dysfunction.[30] Here, we explore whether IH induced pyroptosis of bEnd3 in vitro. The results showed that compared to the NA group, the protein and mRNA expressions of GSDMD and Caspase-1 in bEnd3 cells from IH group were significantly increased (Figure 2A and B). Pyroptosis was associated with the activation of inflammatory response. In this study, ELISA was used to detect the expression of inflammatory factors. The results showed that IL-1β, IL-6, IL-18 and TNF-α in cellular supernatant in IH group were significantly increased compared to those in NA group, and the trend was consistent with pyroptosis (Figure 2C). Moreover, interestingly, our results showed that miR-20a-5p was also increased in the IH group (Figure 2D). These results suggest that IH can induce pyroptosis and promote inflammation in bEnd3 cells. Meanwhile, IH stimulate the expression of miR-20a-5p. As demonstrated in studies, miR-20a-5p plays an important role in the pyroptosis, which may be one of the mechanisms by which OSA induces BBB disruption.

Exosome Characterization and Uptake

Exosomes transmit biological signals between cells. In order to demonstrate that bEnd3-cell-derived exosomes treated with NA or IH are internalized by HT22 cells, the exosomes were first isolated and purified, and then identified by TEM, NTA, and Western blot. TEM showed that exosomes had bilayer membrane and were spherical (Figure 3A). NTA results showed that the diameter of exosomes was mainly between 70 and 120 nm, with a peak value at 100 nm (Figure 3B). Western blot results confirmed the presence of exosome-specific markers such as CD9 and CD63 on the surface of these

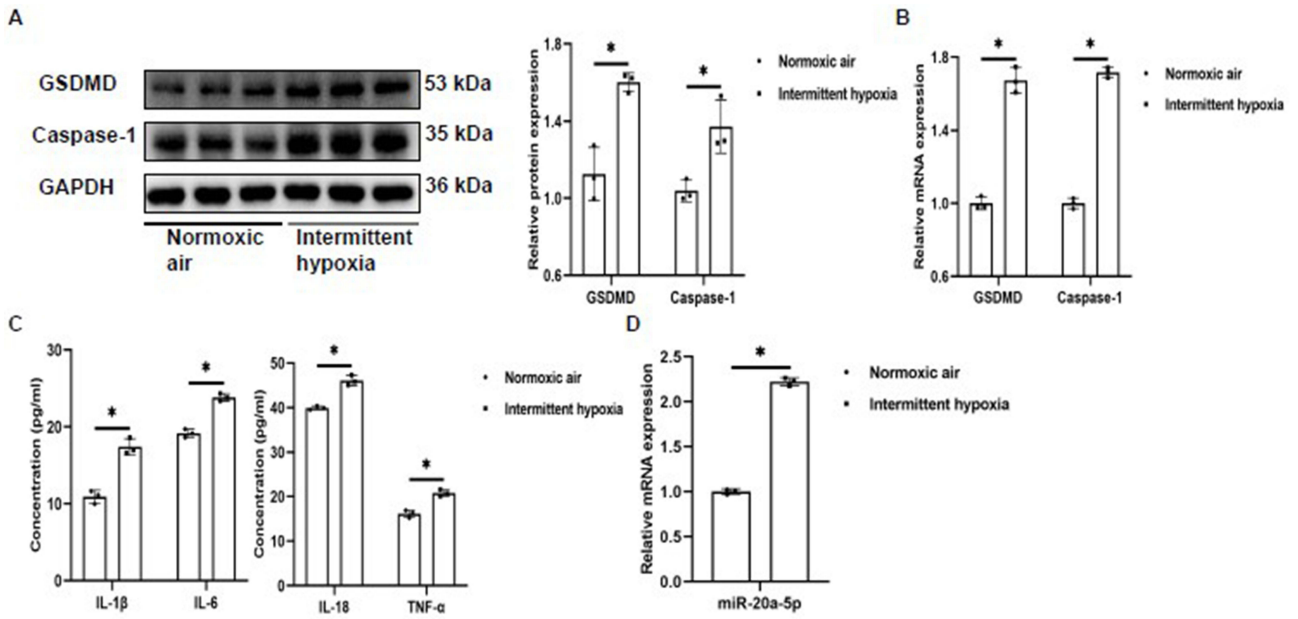

Figure 2 IH promotes pyroptosis and inflammation of bEnd3 cells (n=3). (**A** and **B**) The expression of GSDMD and Caspase-1 protein and mRNA in bEnd3 cells was detected by Western blot and qRT-PCR. (**C**) The levels of IL-1β, IL-6, IL-18, and TNF-α in the supernatant of bEnd3 cells were detected by ELISA. (**D**) The expression of miR-20a-5p in bEnd3 cells was detected by qRT-PCR. Statistical analysis of the data was performed using Student's *t*-test, df=4. **P*<0.05.

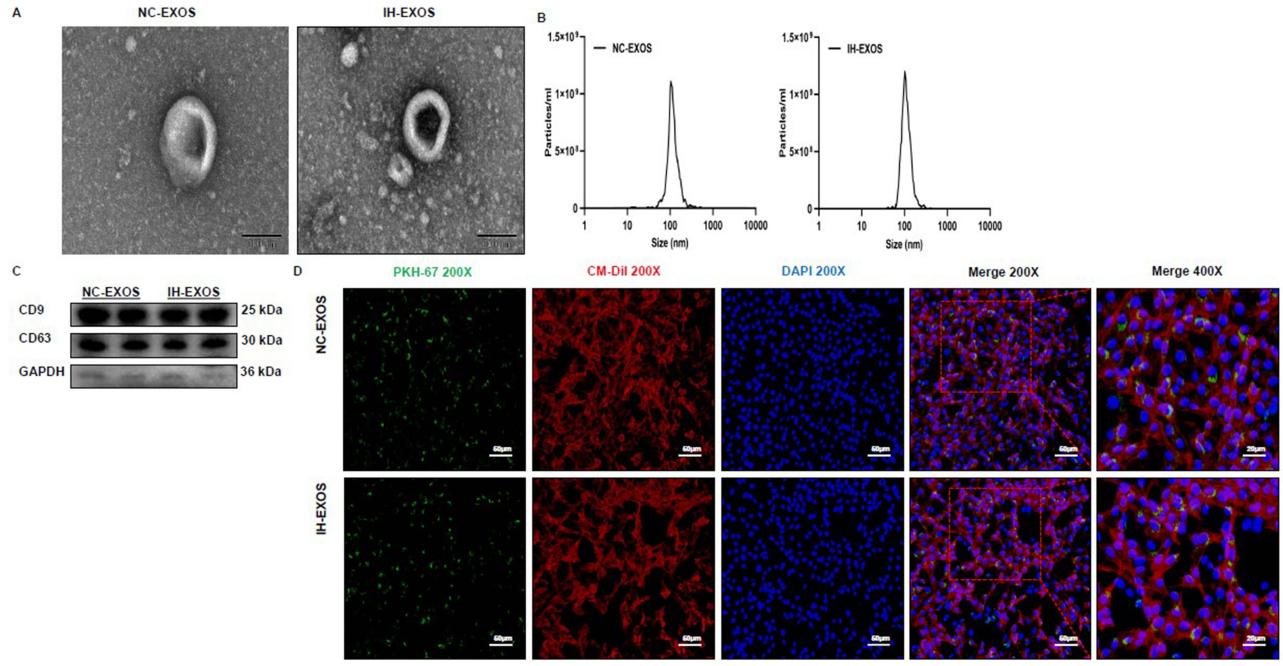

Figure 3 Exosome characterization and uptake (n=3). (**A**) TEM of bEnd3-cell-derived exosomes. Magnification×20000. Scale bar, 100 μm. (**B**) DLS of bEnd3-cell-derived exosomes. (**C**) Western blot of exosomal marker CD9 and CD63 and cell marker GAPDH. (**D**) Fluorescence images of HT22 cells incubated with PKH67-labelled bEnd3-cell-derived exosomes (green). Dil (red) was stained of membrane. Nuclei were stained with DAPI (blue). Magnification×200. Scale bar, 50 μm. Magnification×400. Scale bar, 20 μm.

particles, and the low or no expression of cytoplasmic protein GAPDH in these particles, further confirming that they were exosomes (Figure 3C). The above data prove that these particles are exosomes. To demonstrate the uptake of exosomes by HT22 cells, HT22 cells were co-cultured with PKH67-labeled exosomes, and the exosomes were found to be internalized in HT22 cells (Figure 3D), indicating that the exosomes were functionally intact and entosis might be the main mechanism of the internalization of exosomes in HT22 cells.

IH-Induced Exosomes Promote Pyroptosis and Inflammation in HT22 Cells

Increased pyroptosis has been reported in OSA patients.[31] However, it is unclear whether IH-induced exosomes can cause pyroptosis. For this purpose, IH-EXOS was co-incubated with HT22 cells to detect the expression of pyroptosis. The results showed that compared to the normal control and NC-EXOS groups, the expression levels of GSDMD and Caspase-1 protein and mRNA in HT22 cells of IH-EXOS group were significantly increased. At the same time, the levels of inflammatory cytokines IL-1β, IL-6, IL-18 and TNF-α were significantly increased, which was related to the promotion of inflammatory response by pyroptosis (Figure 4A–C). To confirm that pyroptosis is caused by exosomes, GW4869, a confirmed exosome secretion inhibitor, was added to bEnd3 cells culture medium and the exosomes were isolated, and then co-cultured with HT22 cells. The results showed that GW4869 could reduce the effect of IH-EXOS on HT22 cells, which was demonstrated by the decreased expression levels of GSDMD, Caspase-1 and inflammatory factors (Figure 4A–C). These results suggest that IH-EXOS can induce pyroptosis of HT22 cells and activate the inflammatory response, which may be one of the mechanisms of neuronal cell death.

The Exosomes Secrete miR-20a-5p

Exosomes often contain miRNAs, which are delivered by exosomes to facilitate their communication between cells. It has been reported that miR-20a-5p is involved in the occurrence of pyroptosis,[16] and IH could cause the up-regulation of

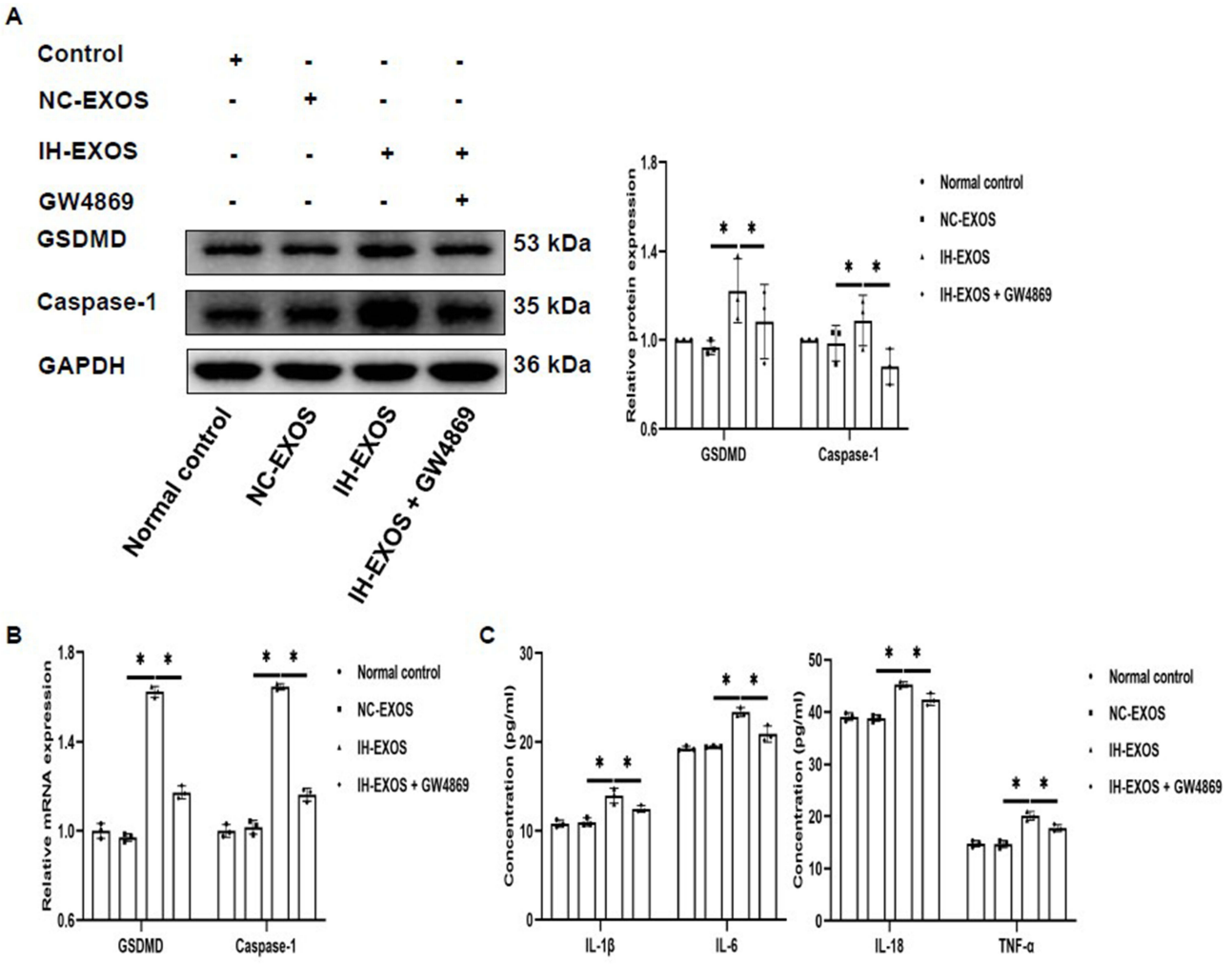

Figure 4 IH-induced exosomes promote pyroptosis and inflammation in HT22 cells (n=3). (**A** and **B**) The expression of GSDMD and Caspase-1 protein and mRNA in HT22 cells was detected by Western blot and qRT-PCR. (**C**) The levels of IL-1β, IL-6, IL-18, and TNF-α in the supernatant of HT22 cells were detected by ELISA. Statistical analysis of the data was performed using one-way ANOVA followed by Bonferroni's multiple comparison tests, *df* (2, 6). **P*<0.05.

miR-20a-5p, so whether miR-20a-5p is expressed in IH-EXOS. In this regard, we used qRT-PCR to detect the expression of miR-20a-5p in exosomes. The results showed that miR-20a-5p in IH-EXOS was significantly higher than that in NC-EXOS (Figure 5A), indicating that IH-EXOS was riched with miR-20a-5p. To determine whether miR-20a-5p was delivered by exosomes, we transfected Cy3-labeled miR-20a-5p mimics (red fluorescence) into bEnd3 cells, isolated exosomes, and then co-cultured them with HT22 cells to track the intercellular transport of miR-20a-5p for communication (Figure 5B). The results showed that HT22 cells showed red fluorescence, indicating that miR-20a-5p transfected into bEnd3 cells was transferred between cells (Figure 5C). These data suggested that miR-20a-5p can be delivered through exosomes. In addition, IH-EXOS co-cultured with HT22 cells also promoted the expression of miR-20a-5p, and when GW4869 blocked the secretion of exosomes derived from bEnd3 cells, the expression of miR-20a-5p was also inhibited (Figure 5D). Taken together, these results suggest that miR-20a-5p is mainly secreted in the form of exosomes, which might be a mechanism of neuroinflammation.

IH-Induced Exosomes Caused Behavior and Cognitive Deficits in Mice

Exosomes also play a role in intracellular communication in vivo, which is crucial for studying the pathogenesis of exosome-mediated OSA-CI. Thus, we injected exosomes or 1xPBS into mice through the tail vein to study the fate of exosomes in vivo (Figure 6A). To confirm the successful injection of exosomes, the exosomes were labeled with PKH67, and tissue testing revealed exosomal green fluorescence in the hippocampus (Figure 6B). OSA can cause CI, and OSA patients' plasma exosomes can destroy the BBB, which may be the basis of CI. To assess the effects of exosomes in vivo, the spatial learning and memory abilities of mice were examined using MWM tests. After training mice to remember the location of the escape platform for 5 consecutive days, it was found that the escape latency was significantly increased in the IH-EXOS group compared to the NC and NC-EXOS groups (Figure 6C). At the same time, memory tests were performed on the mice after the underwater platform was removed. The results showed that the percentage of time spent in the target quadrant and the crossing frequency of the target platform were significantly reduced in the IH-EXOS group compared to the NC and NC-EXOS groups (Figure 6D and E). In addition, mouse swimming tracks showed that mice in the IH-EXOS group remained in the non-target quadrant longer than those in the NC and NC-EXOS groups (Figure 6F). These data suggest that IH-EXOS is taken up by hippocampus in vivo and caused spatial memory and cognitive deficits in mice.

IH-Induced Exosomes Promote Pyroptosis and Inflammation in the Hippocampus in vivo

In this study, IH-EXOS could increase pyroptosis of HT22 cells in vitro. Consequently, an intriguing question arises: Can IH-EXOS also induce pyroptosis in vivo? Histological results showed that hippocampal neurons in the NC and NC-

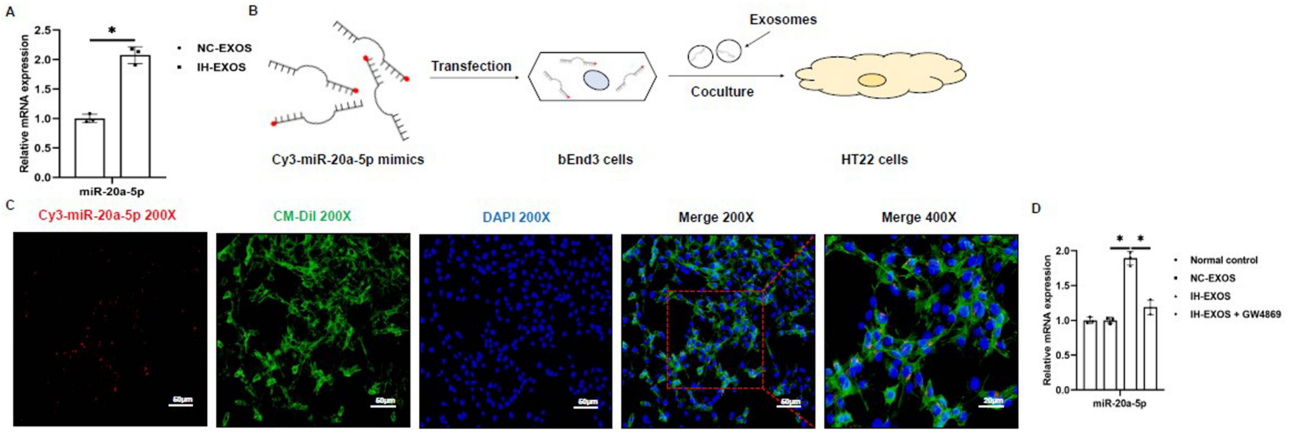

Figure 5 The exosomes secrete miR-20a-5p (n=3). (**A**) The expression of miR-20a-5p in exosomes was detected by qRT-PCR. (**B**) Exosomes isolated from bEnd3 cells transfected with Cy3-labeled miR-20a-5p mimics (red) were co-cultured with HT22 cells. (**C**) Fluorescence images of HT22 cells incubated with exosomes derived from bEnd3 cells transfected with Cy3-miR-20a-5p. Magnification×200. Scale bar, 50 μm. Magnification×400. Scale bar, 20 μm. (**D**) The expression of miR-20a-5p in HT22 cells was detected by qRT-PCR. Statistical analysis of the data was performed using Student's *t*-test ((**A**), df=4), one-way ANOVA (**D**) followed by Bonferroni's multiple comparison tests, *df* (2, 6). *$P<0.05$.

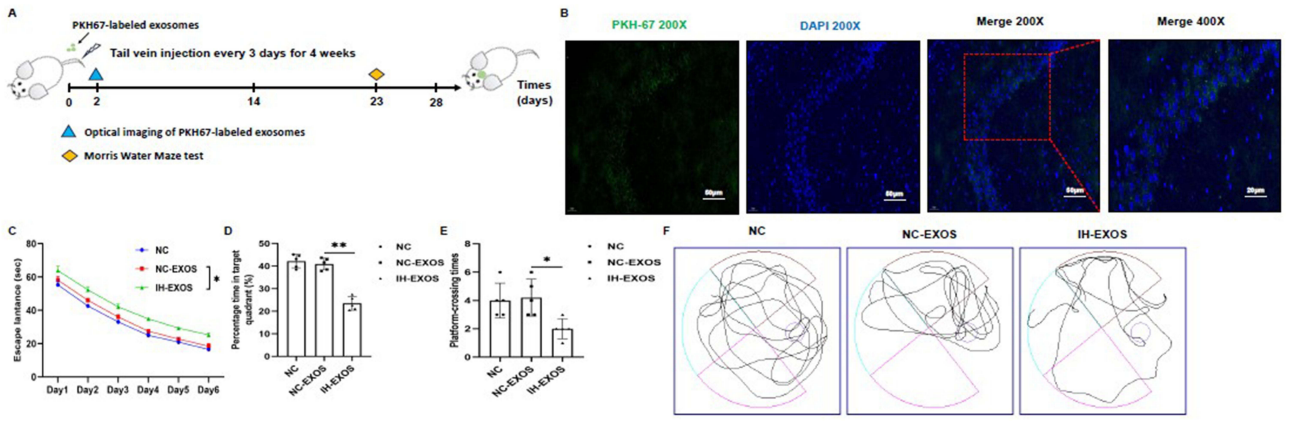

Figure 6 IH-induced exosomes caused behavior and cognitive deficits in mice (n=15). (**A**) Flow diagram of bEnd3-cell-derived exosomes intervention in mice. (**B**) Fluorescence images of PKH67-labelled bEnd3-cell-derived exosomes in hippocampus. Exosomes were labelled with PKH67 (green) and nuclei were stained with DAPI (blue). Magnification×200. Scale bar, 50 μm. Magnification×400. Scale bar, 20 μm. (**C**) Escape latency was the time that mice first climbed onto the hidden platform or first passed through the area where the platform was located. (**D**) The percentage of time that mice spent in the quadrant where the platform is located versus the total time. (**E**) The frequency of passing through the area where the platform was located. (**F**) The swimming trail map of mouse in the swimming pool during 60 seconds at day 6. Statistical analysis of the data was performed using one-way ANOVA (**D** and **E**), and two-way ANOVA (**C**) followed by Bonferroni's multiple comparison tests, *df* (2, 12). **P*<0.05. ***P*<0.01.

EXOS groups had clear nuclei, complete structures, and abundant cytoplasm, while hippocampal neurons in the OSA-EXOS group showed obvious degeneration, structural evacuation, and disappearance of nucleoli (Figure 7A). At the same time, Nissl staining of hippocampal tissue was performed to assess the survival of hippocampal neurons, which showed that the number of hippocampal neurons was significantly reduced in the IH-EXOS group compared to the NC and NC-EXOS groups (Figure 7B). Immunohistochemical analysis of hippocampal tissue showed significantly increased staining of GSDMD and Caspase-1 in IH-EXOS group compared to the NC and NC-EXOS groups (Figure 7C). In addition, the levels of GSDMD and Caspase-1 protein and mRNA in hippocampus were significantly increased, and the expression levels of inflammatory factors IL-1β, IL-6, IL-18, and TNF-α were up-regulated, which triggered inflammation and accelerated neuronal damage, which was consistent with the response induced by IH-EXOS in vitro (Figures 7D–F). As expected, the expression of miR-20a-5p in the hippocampus was increased in the IH-EXOS group, consistent with the response induced by co-incubation of IH-EXOS with HT22 cells in vitro (Figure 7G). These results indicate that IH-EXOS could also communicate in vivo, which was consistent with previous reports. At the same time, IH-EXOS damaged hippocampal neurons in vivo, activating pyroptosis and inflammatory responses that leaded to cognitive deficits in mice, which may be related to the regulation of miR-20a-5p.

The Expression of MFN2 Was Impaired

In order to elucidate the mechanism of pyroptosis induced by miR-20a-5p in HT22 cells, TargetScanHuman8.0 (www.targetscan.org/vert_80/) and miRDB (https://mirdb.org/index.html) were used to predict the target mRNA. Among the potential targets of miR-20a-5p, mitofusin 2 (MFN2) has been studied in pyroptosis, and overexpression of MFN2 has been found to inhibit the expression of GSDMD and Caspase-1 pyroptosis proteins in cells.[32] In this regard, we investigated the role of MFN2 in pyroptosis induced by IH and IH-EXOS. The results showed that in bEnd3 cells, protein and mRNA levels of MFN2 were down-regulated in the IH group (Figure 8A and B). In co-culture of IH-EXOS and HT22 cells, the expression of MFN2 protein and mRNA also decreased (Figure 8C and D). In vivo exosome intervention experiments, compared to the NC and NC-EXOS groups, immunohistochemical analysis of MFN2 and its protein and mRNA levels in IH-EXOS group showed decreased expression (Figure 8E–G). These results suggest that IH and IH-EXOS could cause impaired MFN2 expression, which might inhibit the development of OSA-CI.

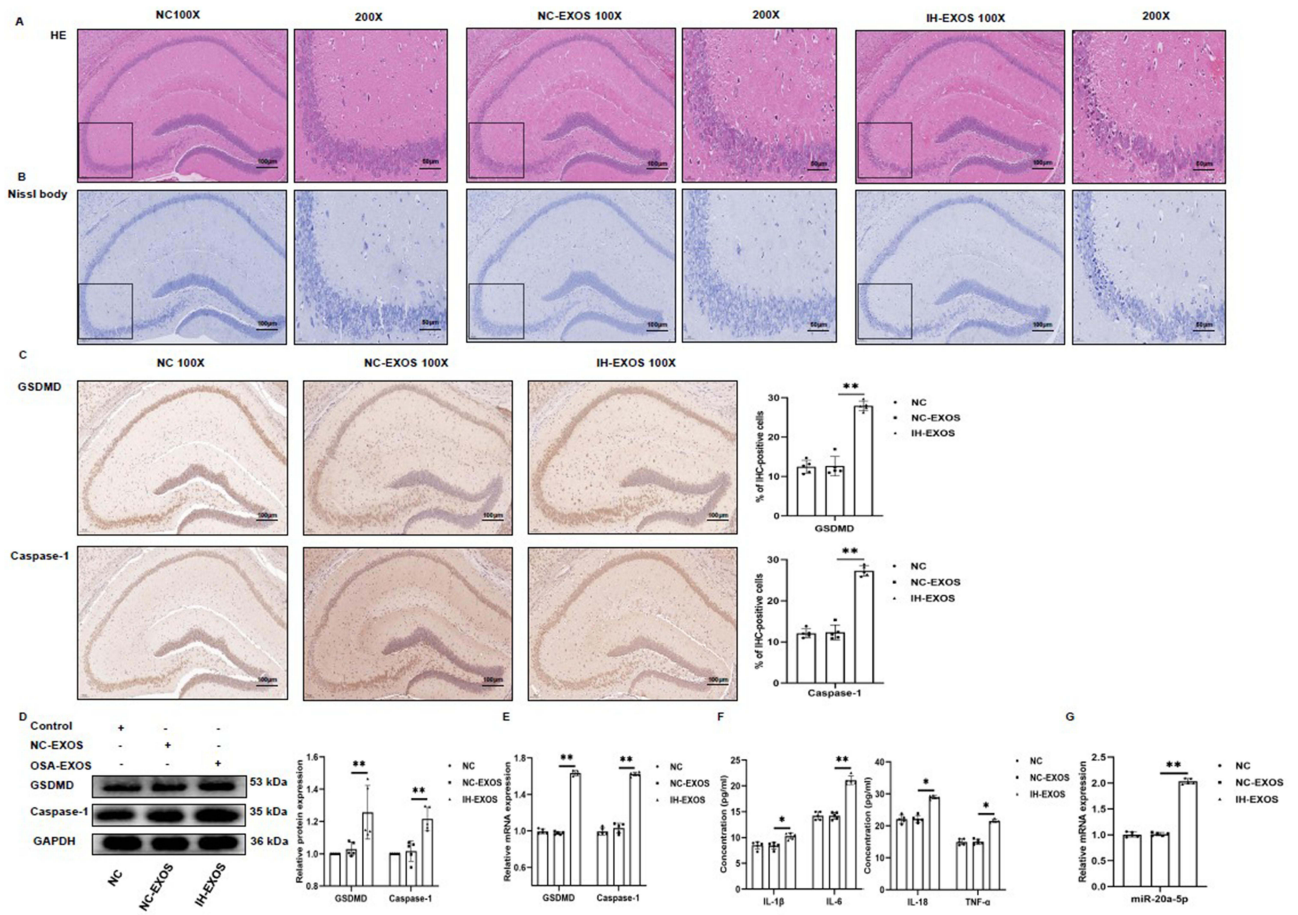

Figure 7 IH-induced exosomes promote pyroptosis and inflammation in the hippocampus in vivo (n=15). (**A**) The hippocampus was stained with H&E to assess pathological changes. (**B**) The hippocampus was stained with Nissl to assess neuronal death. (**C**) The hippocampus was performed with anti-GSDMD and anti-Caspase-1 for immunohistochemical staining. Magnification×100, the scale is 100 μm. Magnification×200, the scale is 50 μm. (**D** and **E**) The expression of GSDMD and Caspase-1 protein and mRNA in the hippocampus was detected by Western blot and qRT-PCR. (**F**) The levels of IL-1β, IL-6, IL-18, and TNF-α in the serum were detected by ELISA. (**G**) The expression of miR-20a-5p in the hippocampus was detected by qRT-PCR. Statistical analysis of the data was performed using one-way ANOVA followed by Bonferroni's multiple comparison tests, *df* (2, 12). **P*<0.05. ***P*<0.01.

Abbreviation: IHC, immunohistochemistry.

Subject Characteristics

Table 2 showed the demographic characteristics and polysomnography parameters of 38 participants, including 18 hCs and 20 severe OSA patients. There were no differences in age, sex, smoking history and years of education between HCs and severe OSA patients. However, BMI, AHI, ODI, and ESS scores were higher in patients with severe OSA compared to HCs. In contrast, HCs had higher LSaO2, MSaO2, and MoCA scores compared to patients with severe OSA. These results suggest that sleepiness, CI, and respiratory impairment were more pronounced in patients with severe OSA than in HCs. Detailed characteristics of volunteers were shown in Table 1.

Correlation Between the Levels of miR-20a-5p, GSDMD, MFN2 and Clinical Features in Patients with Severe OSA

In this study, it was found that IH and IH-EXOS induced pyroptosis and miR-20a-5p increased expression, and decreased MFN2 level, but their roles in the pathogenesis of OSA and their effects on cognitive function have not been reported. To this end, we isolated PBMCs from HCs and severe OSA patients and used qRT-PCR to detect pyroptosis, miR-20a-5p, and MFN2 expression. The results showed that GSDMD, Caspase-1, miR-20a-5p and inflammatory factors were significantly increased in severe OSA compared to the HCs group, while MFN2 was decreased in the opposite way (Figure 9A–D). To determine the role of the above indicators in OSA-CI, correlation analysis was used to evaluate their

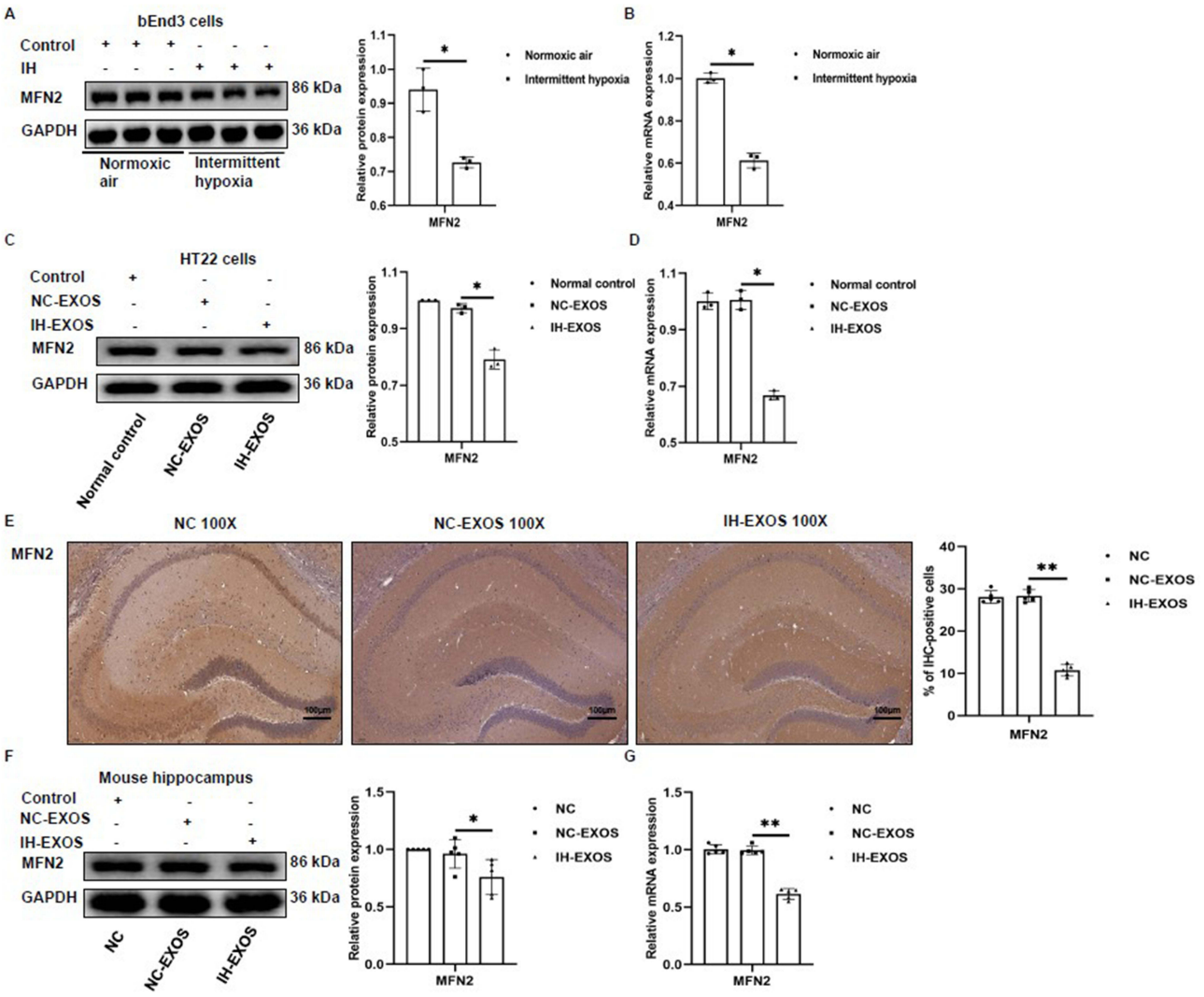

Figure 8 The expression of MFN2 was impaired (n=3). (**A** and **B**) The expression of MFN2 protein and mRNA in bEnd3 cells was detected by Western blot and qRT-PCR. (**C** and **D**) The expression of MFN2 protein and mRNA in HT22 cells was detected by Western blot and qRT-PCR. (**E**) The hippocampus was subjected to anti-MFN2 immunohistochemical staining. Magnification×100, the scale is 100 μm. (**F** and **G**) The expression of MFN2 protein and mRNA in the hippocampus was detected by Western blot and qRT-PCR. Statistical analysis of the data was performed using Student's *t*-test (A and B, df=4), one-way ANOVA [C and D, *df* (2, 6); E-G, *df* (2, 12)] followed by Bonferroni's multiple comparison tests. **P*<0.05. ***P*<0.01.

Abbreviation: IHC, immunohistochemistry.

role in severe OSA. The results showed that in severe OSA group, clinical AHI was positively correlated with GSDMD (r=0.819, P<0.001; Figure 9E) and miR-20a-5p (r=0.653, P=0.002; Figure 9F), but negatively correlated with MFN2 (r=−0.739, P<0.001; Figure 9G) and MoCA (r=−0.736, P<0.001; Figure 9H). In addition, clinical MoCA was negatively correlated with GSDMD (r=−0.479, P=0.032; Figure 9I) and miR-20a-5p (r=−0.584, P=0.007; Figure 9J), but positively correlated with MFN2 (r=0.731, P<0.001; Figure 9K). Interestingly, miR-20a-5p was positively correlated with GSDMD (r=0.476, P=0.034; Figure 9L), but negatively correlated with MFN2 (r=−0.603, P=0.005; Figure 9M). Furthermore, MFN2 was negatively correlated with GSDMD (r=−0.636, P=0.003; Figure 9N). These results suggest that miR-20a-5p, pyroptosis and MFN2 were involved in the development of OSA-CI, and miR-20a-5p may play a catalytic role in OSA induced CI by regulating MFN2.

MFN2 Inhibits Pyroptosis of HT22 Cells

In this study, IH-EXOS induced pyroptosis in HT22 cells, while MFN2 has been reported to inhibit pyroptosis. However, whether MFN2 can inhibit IH-EXOS-induced pyroptosis of HT22 cells remains unclear. In response, we conducted

Table 2 Clinical Characteristics of Participants

Items	HCs	Severe OSA	*P* value
Subjects, n (%)	18	20	
Categorical variables[a]			
Sex, n (%)	20	20	0.503
Male	10 (55.6)	14 (70.0)	
Female	8 (44.4)	6 (30.0)	
Smoking history, n (%)			0.506
Never-smoker	5 (27.8)	8 (40.0)	
Smoker	13 (72.2)	12 (60.0)	
MoCA score, n (%)			<0.001
≥26	16 (88.9)	4 (20.0)	
<26	2 (11.1)	16 (80.0)	
Continuous variables[b]			
Age (y), M ± SD	47.0 ± 4.7	48.7 ± 6.1	0.329
BMI (kg/m^2), M ± SD	23.5 ± 1.3	29.5 ± 2.3	<0.001
Education (y), M ± SD	10.8 ± 3.0	10.0 ± 2.8	0.516
Polysomnography indexes, M ± SD			
AHI (events/h)	3.0 ± 0.8	51.6 ± 13.6	<0.001
ODI (events/h)	2.7 ± 0.9	13.1 ± 9.2	<0.001
$LSaO_2$ (%)	88.2 ± 3.0	63.5 ± 13.4	<0.001
$MSaO_2$ (%)	94.9 ± 0.7	89.3 ± 2.7	<0.001
ESS scores	7.9 ± 2.1	13.8 ± 2.5	<0.001
MoCA scores	26.6 ± 1.1	22.8 ± 3.1	<0.001

Notes: Comparisons were determined using Student's *t*-test and chi-square test or Fisher's precision test between two groups. *P*<0.05 was considered statistically significant. [a]p values from either chi-square test (df=1) or Fisher's exact test, comparing health comparisons (HCs) group and severe OSA group. [b]p values from Student's *t*-test, comparing health comparisons (HCs) group and severe OSA group, df=36.

Abbreviations: AHI, apnea-hypopnea index; BMI, body mass index; ODI, oxygen desaturation index; ESS, Epworth Sleepiness Scale; MoCA, Montreal Cognitive Assessment; $LSaO_2$, lowest oxygen saturation during sleep; $MSaO_2$, mean oxygen saturation during sleep; M±SD, mean ± standard deviation.

experiments with MFN2 gene silencing or overexpression in HT22 cells, exposed or not exposed to IH-EXOS. Initially, we demonstrated successful gene silencing or overexpression of MFN2 in HT22 cells in the presence or absence of IH-EXOS (Figure 10A and B,D and E). We then evaluated the expression of pyroptosis in each group. The results showed the opposite trend. Compared to the control group, the expression levels of GSDMD and Caspase-1 protein and mRNA increased or decreased with MFN2 gene silencing or overexpression (Figure 10A and B,D and E), and the level of inflammation also showed a trend consistent with pyroptosis (Figure 10C and F). These results suggest that MFN2 can inhibit IH-EXOS-induced pyroptosis of HT22 cells, which may play an important role in preventing the occurrence of OSA-CI.

miR-20a-5p Promotes Pyroptosis of HT22 Cells by Mediating IH-EXOS by Targeting MFN2

In this study, IH-EXOS promoted the expression of miR-20a-5p, and MFN2 was predicted to be the target of miR-20a-5p. In order to further explore the role of miR-20a-5p in pyroptosis of HT22 cells, we investigated whether miR-20a-5p and MFN2 were associated in HT22 cells with or without IH-EXOS exposure. The results showed that we demonstrated successful silencing or overexpression of miR-20a-5p with or without exposure to IH-EXOS (Figure 11A and E). We then evaluated the expression of MFN2 and pyroptosis genes in each group. Interestingly, compared to the control group,

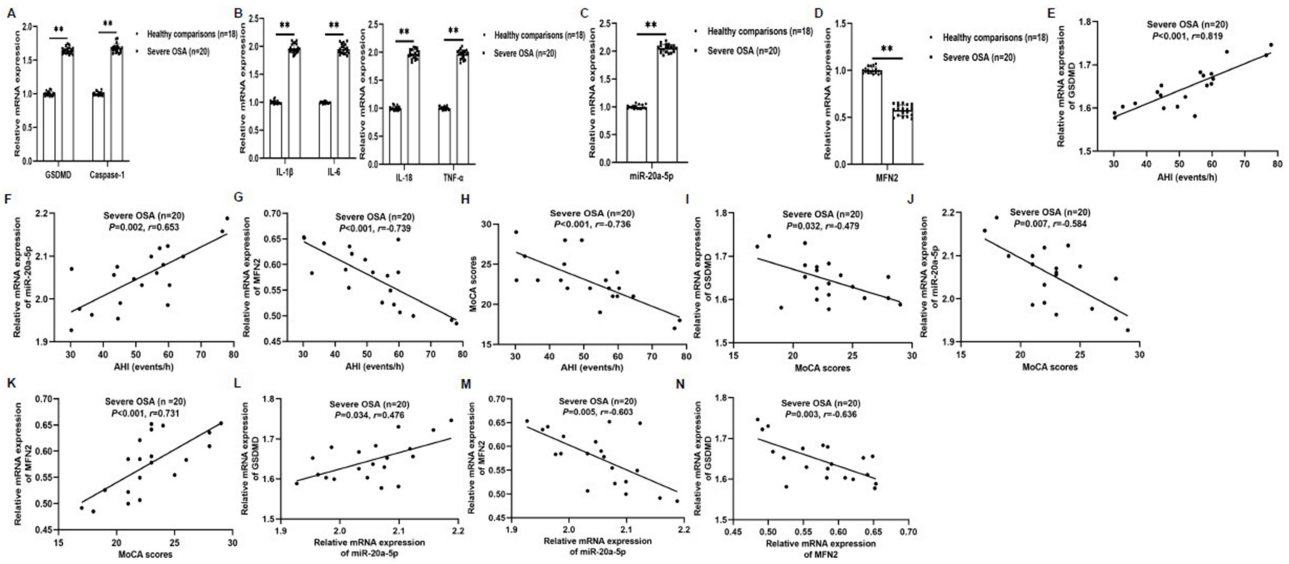

Figure 9 Correlation between the levels of miR-20a-5p, GSDMD, MFN2 and clinical features in patients with severe OSA (n=20). (**A**–**D**) The expression of GSDMD, Caspase-1, IL-1β, IL-6, IL-18, TNF-α, miR-20a-5p, and MFN2 mRNA in peripheral blood was detected by qRT-PCR. (**E**–**H**) The correlation between clinical AHI and GSDMD (**E**), miR-20a-5p (**F**), MFN2 (**G**), and MoCA (**H**). (**I**–**K**) The correlation between clinical MoCA and GSDMD (**I**), miR-20a-5p (**J**), and MFN2 (**K**). (**L** and **M**) The correlation between miR-20a-5p and GSDMD (**L**) and MFN2 (**M**). (**N**) The correlation between MFN2 and GSDMD. Statistical analysis of the data was performed using Student's *t*-test, df=36. Correlations were determined by Spearman's rank correlation test. ***P*<0.01. *P*<0.05 was considered statistically significant.
Abbreviations: AHI, apnea-hypopnea index; MoCA, Montreal Cognitive Assessment.

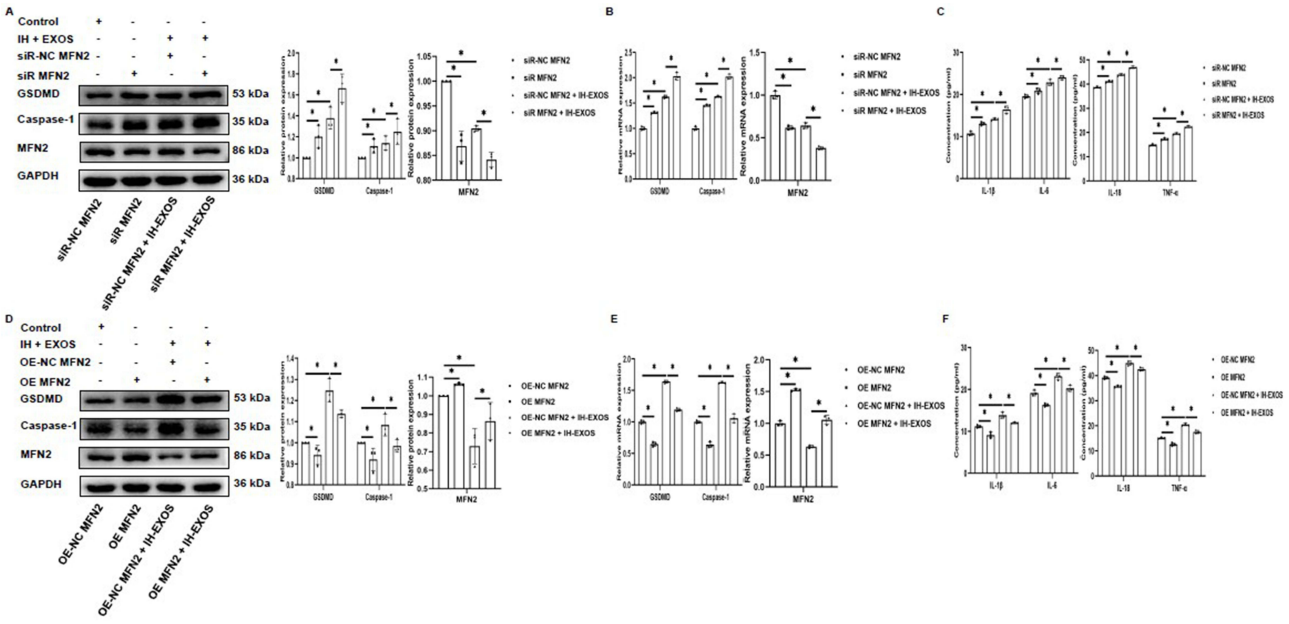

Figure 10 MFN2 inhibits pyroptosis of HT22 cells (n=3). (**A, B, D** and **E**) Western blot and qRT-PCR were used to detect the expression of MFN2, GSDMD, and Caspase-1 protein and mRNA in MFN2 gene silencing or overexpression with or without IH-EXOS exposure. (**C** and **F**) ELISA was used to detect IL-1β, IL-6, IL-18, and TNF-α levels in MFN2 gene silencing or overexpression with or without IH-EXOS exposure. Statistical analysis of the data was performed using two-way ANOVA followed by Bonferroni's multiple comparison tests, *df* (2, 6). **P*<0.05.

MFN2 protein and mRNA expression levels increased or decreased in contrast to miR-20a-5p silenced or overexpressed (Figure 11B and C,F and G). However, GSDMD and Caspase-1 showed a trend consistent with miR-20a-5p silencing or overexpression (Figure 11B and C,F and G). In addition, as expected, levels of inflammatory cytokines also decreased or increased (Figure 11D and H). To further validate MFN2 as a target gene for miR-20a-5p, we performed dual luciferase reporter assays and identified a candidate miR-20a-5p binding site in MFN2 3'UTR (Figure 11I). Luciferase reporter

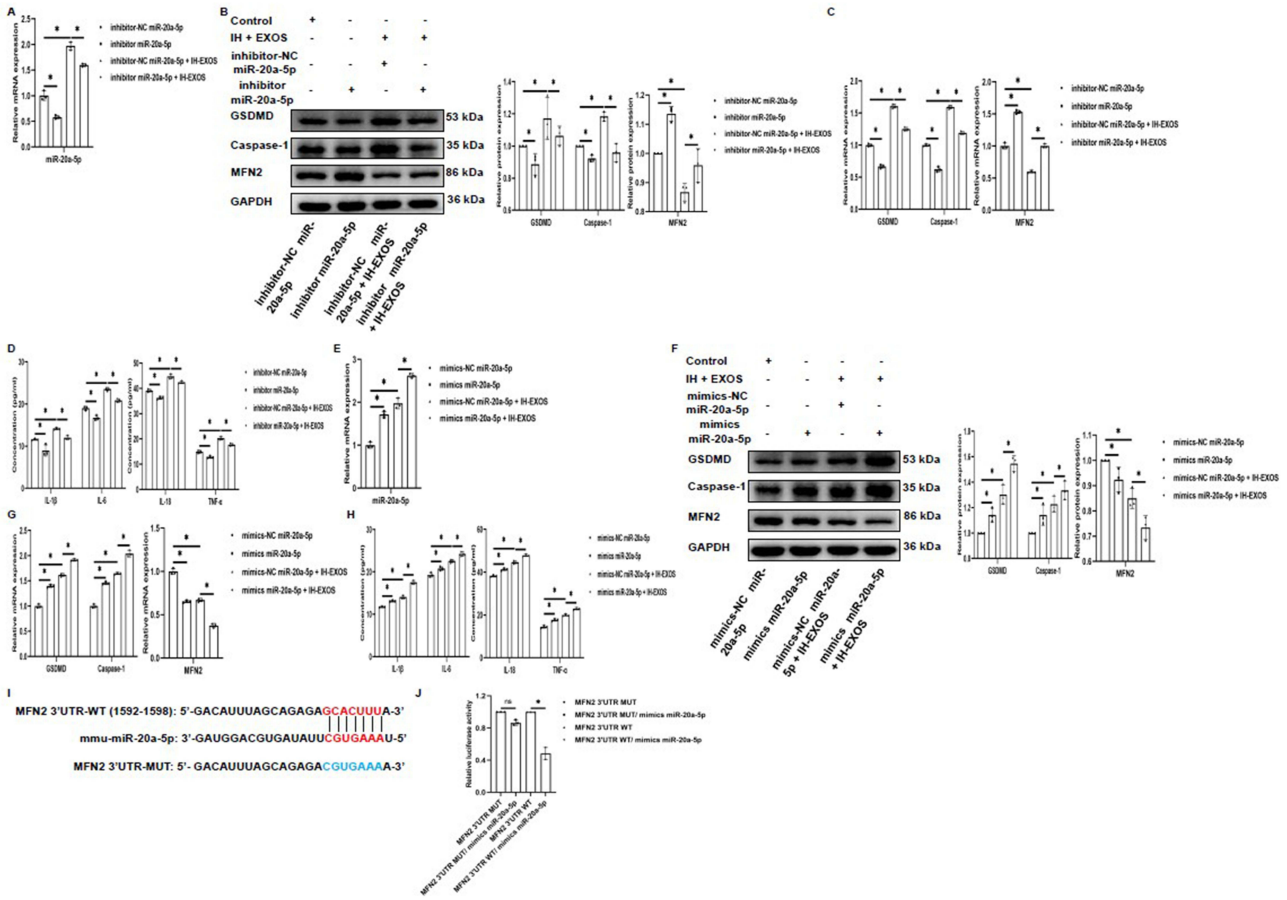

Figure 11 miR-20a-5p promotes pyroptosis of HT22 cells by mediating IH-EXOS by targeting MFN2 (n=3). (**A** and **E**) qRT-PCR was used to detect the expression of miR-20a-5p in miR-20a-5p silencing or overexpression with or without IH-EXOS exposure. (**B, C, F** and **G**) Western blot and qRT-PCR were used to detect the expression of MFN2, GSDMD, and Caspase-1 protein and mRNA in miR-20a-5p silencing or overexpression with or without IH-EXOS exposure. (**D** and **H**) ELISA was used to detect IL-1β, IL-6, IL-18, and TNF-α levels in miR-20a-5p silencing or overexpression with or without IH-EXOS exposure. (**I**) Prediction of interactions between miR-21-3p and its putative binding sites in the 3'UTR of MFN2. (**J**) After co-transfection of miR-20a-5p mimics and MFN2 WT or MUT reporter plasmids for 48h, luciferase activity in HEK293T cells was evaluated and normalized. Statistical analysis of the data was performed using two-way ANOVA followed by Bonferroni's multiple comparison tests, *df* (2, 6). **P*<0.05.

Abbreviations: WT, wild type; MUT, mutant type.

gene vectors containing the WT or MUT version MFN2 3'UTR sequence were transfected into 293T cells together with miR-20a-5p mimics or control mimics. When cells in WT group were transfected with miR-20a-5p mimics, luciferase activity decreased. On the contrary, luciferase activity did not change in the MUT group (Figure 11J). These results suggest that miR-20a-5p promoted pyroptosis of HT22 cells by mediating IH-EXOS by targeting MFN2, and causing or even exacerbating OSA-CI.

Overexpressing MFN2 Can Reverse IH-EXOS-Mediated Pyroptosis of HT22 Cells Induced by miR-20a-5p

Previously, we demonstrated that MFN2 is the target gene of miR-20a-5p. Then, whether MFN2 could reverse the pyroptosis induced by miR-20a-5p on HT22 cells. To do this, we cotransfected HT22 cells with miR-20a-5p mimics and MFN2 gene silencing or overexpression with or without IH-EXOS exposure. The results showed that miR-20a-5p was successfully overexpressed in HT22 cells with IH-EXOS exposure, while MFN2 gene silence or overexpression had no effect on the expression of miR-20a-5p (Figure 12A). Meanwhile, the detection results of MFN2 expression showed that when miR-20a-5p was overexpressed, the expression level of MFN2 was significantly lower than that of the control group when MFN2 was silenced, while the expression level of MFN2 was significantly higher when MFN2 was overexpressed (Figure 12B and C). Interestingly, the expression levels of GSDMD, Caspase-1 and inflammatory factors

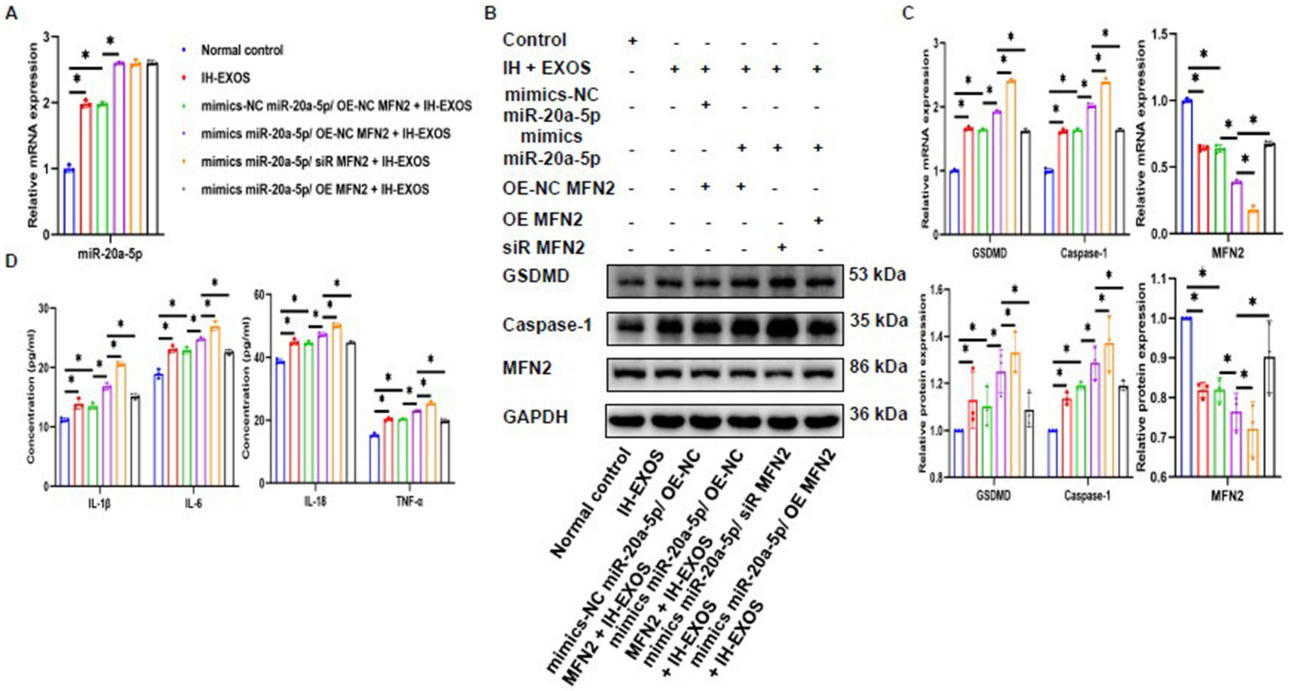

Figure 12 Overexpressing MFN2 can reverse IH-EXOS-mediated pyroptosis of HT22 cells induced by miR-20a-5p (n=3). Following co-transfection of miR-20a-5p mimics and MFN2 silencing or overexpression with or without IH-EXOS exposure, cells were analyzed via (**A**) qRT-PCR was used to detect the expression of miR-20a-5p. (**B** and **C**) Western blot and qRT-PCR were used to detect the expression of MFN2, GSDMD, and Caspase-1 protein and mRNA. (**D**) ELISA was used to detect IL-1β, IL-6, IL-18, and TNF-α levels. Statistical analysis of the data was performed using two-way ANOVA followed by Bonferroni's multiple comparison tests, *df* (5, 12). **P*<0.05.

were significantly higher in the co-transfection of miR-20a-5p mimics and siR MFN2 than in the control group. However, when miR-20a-5p mimics were co-transfected with OE MFN2, the levels of GSDMD, Caspase-1 and inflammatory factors was significantly reduced (Figure 12B–D). These data further suggest that MFN2 is a direct target gene of miR-20a-5p that inhibits the pyroptosis of HT22 cells induced by IH-EXOS, and that overexpression of MFN2 could reverse the pyroptosis of HT22 cells induced by miR-20a-5p in IH-EXOS.

Discussion

This study shows that IH exposure regulates the intercellular communication between bEnd3 cells and HT22 cells, promoting pyroptosis and inflammatory response in HT22 cells through the targeting of MFN2 by exosome miR-20a-5p, thereby accelerating the progression of OSA-CI. Therefore, targeting miR-20a-5p or combining with existing diagnostic and treatment techniques may be a new therapeutic strategy for OSA-CI.

OSA can promote the occurrence of CI, which is related to the damage of hippocampus and BBB caused by IH.[4,6] The study found that adult rats exposed to IH for 14 days showed CI, with a sevenfold to eightfold increase in apoptosis in the CA-1 hippocampus and cortical regions after 1 to 2 days of IH.[33] Pyroptosis, triggers the activation of classical Caspase-1, lysis and activation of GSDMD under adverse environmental conditions, thus causing inflammatory storms, leading to the progression or even deterioration of the disease.[34] In this study, our clinical results showed that CI occurs in severe OSA patients and is negatively correlated with AHI and pyroptosis. It has been reported that the expression of pyroptosis is increased in OSA, while the memory function of mice is significantly improved when pyroptosis is damaged in AD.[9,10] Wu et al discovered that IH could decrease miR-223-3p levels and augment pyroptosis, whereas overexpression of miR-223-3p could mitigate pyroptosis and neuroinflammation induced by IH.[35] BEnd3 cells are an important part of BBB. In this study, it was found that IH can induce pyroptosis of bEnd3 cells and increase the release of inflammatory factors, which is consistent with the previous report, IH can destroy the integrity of BBB and promote the occurrence of OSA-CI.[6] However, according to our analysis, these studies are insufficient and the mechanism by which pyroptosis promotes OSA-CI is not yet understood. Therefore, in our study, better supplementation of IH can cause the

damage of BBB and promote the damage of hippocampal neurons through the secretion of exosomes, resulting in the occurrence of OSA-CI.

Studies have shown that in OSA patients, hypoxia damages the hippocampal region involved in learning and memory.[4] Khalyfa et al found that OSA plasma exosomes can destroy the integrity of BBB, resulting in neuronal cell damage.[15] At present, there are few studies on the exosome sources of IH stimulation, to elucidate the intercellular and in vivo communication role of IH-EXOS, we studied IH-EXOS in vitro and in vivo. The results showed that fluorescently labeled exosomes showed up in HT22 cells and hippocampal tissue, and IH-EXOS significantly promoted pyroptosis and inflammatory factor expression in HT22 cells and hippocampal tissue, and caused spatial memory and behavior impairment in mice. These results indicated that IH damages BBB while stimulating its secretion of harmful exosomes, which can cause damage to hippocampal neurons by inducing pyroptosis and inflammatory response, so as to promote CI. Kim et al found that in a model of post-stroke CI caused by middle cerebral artery occlusion/reperfusion, inflammasome-induced pyroptosis can lead to acute and chronic neuronal death after stroke, and lead to impaired learning and memory function.[36] It has been reported that OSA plasma can cause tumor cell proliferation and migration, cardiovascular dysfunction, and endothelial cell senescence.[37–40] In AD studies, it was found that exosomal neurogranin, synaptosome-associated protein 25 and synaptic binding protein 1 can be used as effective biomarkers to identify CI, further indicating that exosomes are risk factors for the development of CI.[41] It has been reported that IH-induced exosomes are pathogenic and can accelerate cardiomyocyte apoptosis and promote the progression of lung adenocarcinoma.[42,43] However, at present, there are few studies on IH-induced EXOS for inducing CI, which needs to be further explored.

As an intercellular communication carrier, exosomes can transfer a large number of miRNAs contained to the recipient cell, and then bind to the 3'UTR sequence of the target mRNA in the recipient cell to regulate the expression of the target gene.[44] Jiao et al found that exosomes miRNAs can promote cell pyroptosis.[45] It has been reported that miR-20a-5p has a regulatory effect on lipopolysaccharide-induced pyroptosis.[16] Our results suggested that IH could promote the expression of miR-20a-5p in bEnd3, which was then secreted into HT22 cells in exosomes, thus promoting pyroptosis and inflammatory response of HT22 cells. It has been found that miR-20a-5p is related to accelerating the proliferation and migration of various cancers.[46–48] It has also been reported that miR-20a-5p is related to the occurrence of AD and CI.[17,49] TargetScan and miRDB predicted the possible mRNA target of miR-20a-5p. Our experiment confirmed MFN2 as the downstream target of miR-20a-5p and found that MFN2 showed decreased expression under IH and IH-EXOS exposure, which could inhibit the expression of pyroptosis in HT22 cells. MFN2 has been reported to be involved in regulating the occurrence of pyroptosis, inhibiting endothelial inflammation and the progression of clear cell renal cell carcinoma.[32,50,51] Li et al found that cannabidiol improved anxiety response and cognitive deficits in mice in an experimental autoimmune encephalomyelitis model through MFN2.[52] In summary, our study suggests that IH regulates HT22 cell pyroptosis by targeting MFN2 through bEnd3 cell-derived exosomal miR-20a-5p, thereby promoting the progression of OSA-CI. The clinical applicability of targeting miR-20a-5p and MFN2 warrants further exploration, which could potentially guide the development of novel therapeutic strategies.

There were some limitations in this study: (a) This study was a single-center case-control study with patients from one region and an insufficient sample size; therefore, the results of the study might not be representative of the whole country. (b) In this study, MFN2 was investigated as the target of miR-20a-5p, and additional potential targets of miR-20a-5p will need to be further explored through RNA sequencing in the future. (c) We found that MFN2 expression is reduced in OSA patients, and it is meaningful to further explore the underlying mechanisms, such as by constructing gene knockout mice.

Conclusions

In conclusion, this study revealed the intercellular communication between IH-stimulated bEnd3 cells and HT22 cells, promoting OSA-CI. Thus, our study reveals a novel mechanism of IH-induced OSA-CI: IH increases HT22 cells pyroptosis via the previously undescribed bEnd3 cells → exosomal miR-20a-5p → MFN2 pathway (Figure 13). More importantly, this essential communication of exosomes connecting bEnd3 cells and HT22 cells may provide new

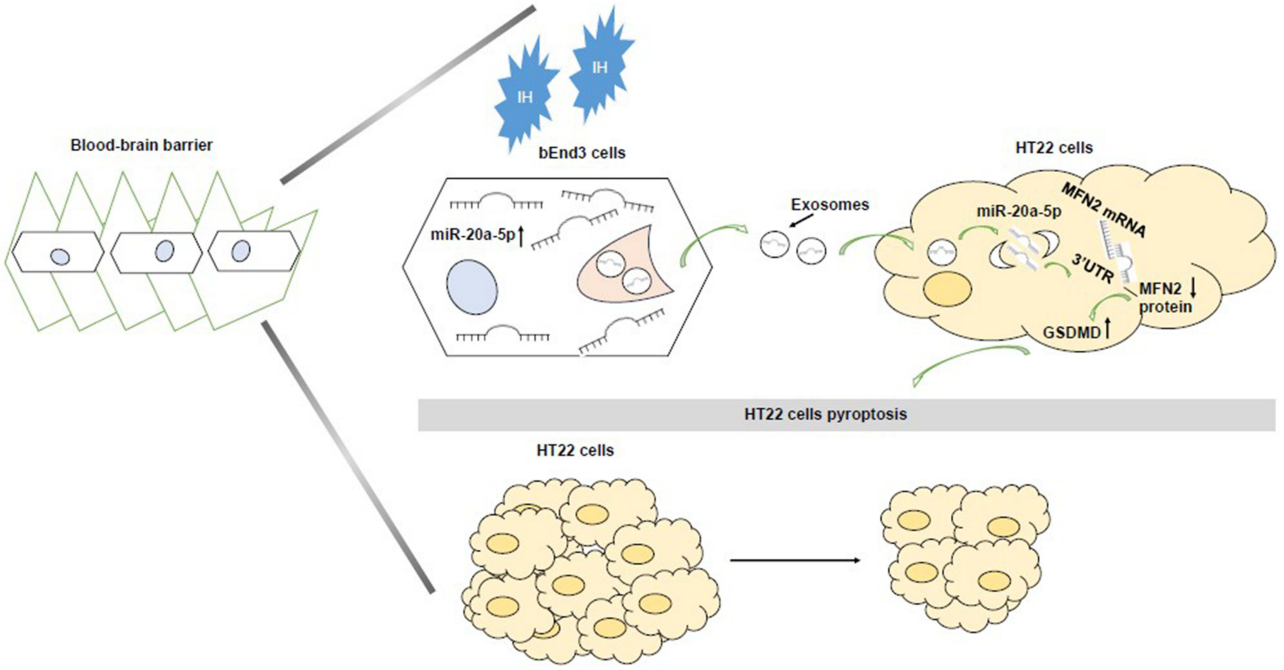

Figure 13 The schematic outlines the mechanistic basis of the observational findings. bEnd3-cell-derived miR-20a-5p stimulated by intermittent hypoxia (IH) is delivered via exosomes to HT22 cells, where it increases pyroptosis of HT22 cells by regulating the MFN2 pathway.

strategies for future prophylactic therapy and may provide new diagnostic and therapeutic techniques for OSA-CI patients.

Data Sharing Statement

The data used to support the findings of this study are included within the article.

Ethics Statement

The Ethics Committee of the Second Xiangya Hospital of Central South University approved this study (Ethical Code: LYF2023059), all subjects signed an informed consent form, and all experiments were conducted in accordance with the Declaration of Helsinki. The animal experiment procedure was approved by the Animal Care and Use Committee of Central South University and was carried out in accordance with the prescribed guiding principles (Ethical Code: CSU-2022-0642).

Innovation Statement

We previously found that plasma-derived exosomes in OSA patients can increase the pyroptosis of hippocampal neurons in mice and impair their spatial memory and learning ability. Through miRNA sequencing, unique miRNA profiles were identified in plasma-derived exosomes of severe OSA, including miR-20a-5p (PMID: 38290937). In this study, we show that intermittent hypoxia of endothelium-derived exosomes causes neuronal pyroptosis and increases cognitive impairment in mice. Given the previously discovered miRNA profile of OSA plasma-derived exosomes and the involvement of miR-20a-5p in the pathogenesis of pyroptosis and Alzheimer's disease, our aim was to investigate the pathogenesis of OSA-related cognitive impairment mediated by intermittent hypoxia-derived exosomes.

Acknowledgments

We thank all the voluntary patients involved in the study.

Funding

This study was supported by the National Natural Science Foundation of China (No. 81970086, No. 82001490, No. 82100039, No. 82170039, No.82300116), the National Key Clinical Specialty Construction Projects of China, the Natural Science Foundation of Hunan Province (No.2023JJ40878), the Natural Science Foundation of Changsha City (CN) (No. kq2208304), and the China Scholarship Council (202406370116).

Disclosure

The authors declare that they have no competing interests.

References

1. Joosten SA, Landry SA, Wong AM, et al. Assessing the physiologic endotypes responsible for REM- and NREM-based OSA. *Chest*. 2021;159(5):1998–2007. doi:10.1016/j.chest.2020.10.080
2. Lutsey PL, Misialek JR, Mosley TH, et al. Sleep characteristics and risk of dementia and Alzheimer's disease: the atherosclerosis risk in communities study. *Alzheimers Dement*. 2018;14(2):157–166. doi:10.1016/j.jalz.2017.06.2269
3. Jorge C, Targa A, Benítez ID, et al. Obstructive sleep apnoea and cognitive decline in mild-to-moderate Alzheimer's disease. *Europ resp J*. 2020;56(5):2000523. doi:10.1183/13993003.00523-2020
4. Olaithe M, Bucks RS, Hillman DR, Eastwood PR. Cognitive deficits in obstructive sleep apnea: insights from a meta-review and comparison with deficits observed in COPD, insomnia, and sleep deprivation. *Sleep Med*. 2018;38:39–49. doi:10.1016/j.smrv.2017.03.005
5. Abbott NJ, Rönnbäck L, Hansson E. Astrocyte-endothelial interactions at the blood-brain barrier. *Nat Rev Neurosci*. 2006;7(1):41–53. doi:10.1038/nrn1824
6. Kim LJ, Martinez D, Fiori CZ, Baronio D, Kretzmann NA, Barros HM. Hypomyelination, memory impairment, and blood-brain barrier permeability in a model of sleep apnea. *Brain Res*. 2015;1597:28–36. doi:10.1016/j.brainres.2014.11.052
7. Schmid-Burgk JL, Gaidt MM, Schmidt T, Ebert TS, Bartok E, Hornung V. Caspase-4 mediates non-canonical activation of the NLRP3 inflammasome in human myeloid cells. *Eur J Immunol*. 2015;45(10):2911–2917. doi:10.1002/eji.201545523
8. Frank D, Vince JE. Pyroptosis versus necroptosis: similarities, differences, and crosstalk. *Cell Death Differ*. 2019;26(1):99–114.
9. Han C, Guo L, Yang Y, et al. Mechanism of microRNA-22 in regulating neuroinflammation in Alzheimer's disease. *Brain Behav*. 2020;10(6):e01627. doi:10.1002/brb3.1627
10. Yu LM, Zhang WH, Han XX, et al. Hypoxia-induced ROS contribute to myoblast pyroptosis during obstructive sleep apnea via the NF- κ B/HIF-1 α signaling pathway. *Oxid Med Cell Longev*. 2019;2019:4596368. doi:10.1155/2019/4596368
11. Kalluri R, LeBleu VS. The biology, function, and biomedical applications of exosomes. *Science*. 2020;367:6478. doi:10.1126/science.aau6977
12. Sun Z, Shi K, Yang S, et al. Effect of exosomal miRNA on cancer biology and clinical applications. *Mol Cancer*. 2018;17(1):147. doi:10.1186/s12943-018-0897-7
13. Parvin R, Zhang L, Zu Y, Ye F. photothermal responsive digital polymerase chain reaction resolving exosomal microRNAs expression in liver cancer. *Small*. 2023;19(28):e2207672. doi:10.1002/smll.202207672
14. Khalyfa A, Kheirandish-Gozal L, Bhattacharjee R, Khalyfa AA, Gozal D. Circulating microRNAs as potential biomarkers of endothelial dysfunction in obese children. *Chest*. 2016;149(3):786–800. doi:10.1378/chest.15-0799
15. Khalyfa A, Gozal D, Kheirandish-Gozal L. Plasma exosomes disrupt the blood-brain barrier in children with obstructive sleep apnea and neurocognitive deficits. *Am J Respir Crit Care Med*. 2018;197(8):1073–1076. doi:10.1164/rccm.201708-1636LE
16. Deng LT, Wang QL, Yu C, Gao M. lncRNA PVT1 modulates NLRP3-mediated pyroptosis in septic acute kidney injury by targeting miR-20a-5p. *Mol Med Rep*. 2021;23(4). doi:10.3892/mmr.2021.11910
17. Wang L, Zhen H, Sun Y, et al. Plasma exo-miRNAs correlated with ad-related factors of Chinese individuals involved in Aβ accumulation and cognition decline. *Mol Neurobiol*. 2022;59(11):6790–6804. doi:10.1007/s12035-022-03012-0
18. Chen Z, Shang Y, Ou Y, et al. Obstructive sleep apnea plasma-derived exosomes mediate cognitive impairment through hippocampal neuronal cell pyroptosis. *Am J Geriatr Psychiatry*. 2024;32(8):922–939. doi:10.1016/j.jagp.2024.01.017
19. Liu W, Zhang W, Wang T, et al. Obstructive sleep apnea syndrome promotes the progression of aortic dissection via a ROS- HIF-1α-MMPs associated pathway. *Int J Bio Sci*. 2019;15(13):2774–2782. doi:10.7150/ijbs.34888
20. Li P, Kaslan M, Lee SH, Yao J, Gao Z. Progress in exosome isolation techniques. *Theranostics*. 2017;7(3):789–804. doi:10.7150/thno.18133
21. Zhu J, Liu B, Wang Z, et al. Exosomes from nicotine-stimulated macrophages accelerate atherosclerosis through miR-21-3p/PTEN-mediated VSMC migration and proliferation. *Theranostics*. 2019;9(23):6901–6919. doi:10.7150/thno.37357
22. Zhai L, Shen H, Sheng Y, Guan Q. ADMSC exo-MicroRNA-22 improve neurological function and neuroinflammation in mice with Alzheimer's disease. *J Cell Mol Med*. 2021;25(15):7513–7523. doi:10.1111/jcmm.16787
23. Gao H, Han Z, Huang S, et al. Intermittent hypoxia caused cognitive dysfunction relate to miRNAs dysregulation in hippocampus. *Behav Brain Res*. 2017;335:80–87. doi:10.1016/j.bbr.2017.06.025
24. Feltner C, Wallace IF, Aymes S, et al. Screening for obstructive sleep apnea in adults: updated evidence report and systematic review for the us preventive services task force. *JAMA*. 2022;328(19):1951–1971. doi:10.1001/jama.2022.18357
25. Corral J, Sánchez-Quiroga M, Carmona-Bernal C, et al. Conventional polysomnography is not necessary for the management of most patients with suspected obstructive sleep apnea. noninferiority, randomized controlled trial. *Am J Respir Crit Care Med*. 2017;196(9):1181–1190. doi:10.1164/rccm.201612-2497OC
26. Kapur VK, Auckley DH, Chowdhuri S, et al. Clinical practice guideline for diagnostic testing for adult obstructive sleep apnea: an American Academy of Sleep Medicine clinical practice guideline. *J Clin Sleep Med*. 2017;13(3):479–504. doi:10.5664/jcsm.6506
27. Walker NA, Sunderram J, Zhang P, Lu SE, Scharf MT. Clinical utility of the Epworth sleepiness scale. *Sleep Breath*. 2020;24(4):1759–1765. doi:10.1007/s11325-020-02015-2

28. Jia X, Wang Z, Huang F, et al. A comparison of the Mini-Mental State Examination (MMSE) with the Montreal Cognitive Assessment (MoCA) for mild cognitive impairment screening in Chinese middle-aged and older population: a cross-sectional study. *BMC Psychiatry*. 2021;21(1):485. doi:10.1186/s12888-021-03495-6
29. Tang FS, Hansbro PM, Burgess JK, Ammit AJ, Baines KJ, Oliver BG. A novel immunomodulatory function of neutrophils on rhinovirus-activated monocytes in vitro. *Thorax*. 2016;71(11):1039–1049. doi:10.1136/thoraxjnl-2015-207781
30. Wei C, Jiang W, Wang R, et al. Brain endothelial GSDMD activation mediates inflammatory BBB breakdown. *Nature*. 2024;629(8013):893–900. doi:10.1038/s41586-024-07314-2
31. Díaz-García E, Sanz-Rubio D, García-Tovar S, et al. Inflammasome activation mediated by oxidised low-density lipoprotein in patients with sleep apnoea and early subclinical atherosclerosis. *Europ Resp J*. 2023;61(3):2201401. doi:10.1183/13993003.01401-2022
32. Kai J, Yang X, Wang Z, et al. Oroxylin a promotes PGC-1α/Mfn2 signaling to attenuate hepatocyte pyroptosis via blocking mitochondrial ROS in alcoholic liver disease. *Free Radic Biol Med*. 2020;153:89–102. doi:10.1016/j.freeradbiomed.2020.03.031
33. Gozal D, Daniel JM, Dohanich GP. Behavioral and anatomical correlates of chronic episodic hypoxia during sleep in the rat. *J Neurosci*. 2001;21(7):2442–2450. doi:10.1523/JNEUROSCI.21-07-02442.2001
34. Boucher D, Monteleone M, Coll RC, et al. Caspase-1 self-cleavage is an intrinsic mechanism to terminate inflammasome activity. *J Exp Med*. 2018;215(3):827–840. doi:10.1084/jem.20172222
35. Wu C, Xing W, Zhang Y, et al. NLRP3/miR-223-3p axis attenuates neuroinflammation induced by chronic intermittent hypoxia. *Funct Integr Genomics*. 2023;23(4):342. doi:10.1007/s10142-023-01268-w
36. Kim H, Seo JS, Lee SY, et al. AIM2 inflammasome contributes to brain injury and chronic post-stroke cognitive impairment in mice. *Brain Behav Immunity*. 2020;87:765–776. doi:10.1016/j.bbi.2020.03.011
37. Almendros I, Khalyfa A, Trzepizur W, et al. Tumor cell malignant properties are enhanced by circulating exosomes in sleep apnea. *Chest*. 2016;150(5):1030–1041. doi:10.1016/j.chest.2016.08.1438
38. Khalyfa A, Trzepizur W, Gileles-Hillel A, et al. Heterogeneity of melanoma cell responses to sleep apnea-derived plasma exosomes and to intermittent hypoxia. *Cancers*. 2021;13(19):4781. doi:10.3390/cancers13194781
39. Khalyfa A, Zhang C, Khalyfa AA, et al. Effect on intermittent hypoxia on plasma exosomal micro RNA signature and endothelial function in healthy adults. *Sleep*. 2016;39(12):2077–2090. doi:10.5665/sleep.6302
40. Khalyfa A, Marin JM, Qiao Z, Rubio DS, Kheirandish-Gozal L, Gozal D. Plasma exosomes in OSA patients promote endothelial senescence: effect of long-term adherent continuous positive airway pressure. *Sleep*. 2020;43(2). doi:10.1093/sleep/zsz217
41. Jia L, Zhu M, Kong C, et al. Blood neuro-exosomal synaptic proteins predict Alzheimer's disease at the asymptomatic stage. *Alzheimers Dement*. 2021;17(1):49–60. doi:10.1002/alz.12166
42. Xie HS, Huang JF, Lin QX, Chen YW, Chen GP, Lin QC. The role of exosomal circular RNA ZNF292 in intermittent hypoxia-induced AC16 cardiomyocytes injury. *Sleep Breath*. 202328:319-–329.
43. Ren J. Intermittent hypoxia BMSCs-derived exosomal miR-31-5p promotes lung adenocarcinoma development via WDR5-induced epithelial mesenchymal transition. *Sleep Breath*. 2023;27(4):1399–1409. doi:10.1007/s11325-022-02737-5
44. Bartel DP. MicroRNAs: genomics, biogenesis, mechanism, and function. *Cell*. 2004;116(2):281–297. doi:10.1016/S0092-8674(04)00045-5
45. Jiao Y, Zhang T, Zhang C, et al. Exosomal miR-30d-5p of neutrophils induces M1 macrophage polarization and primes macrophage pyroptosis in sepsis-related acute lung injury. *Critical Care*. 2021;25(1):356. doi:10.1186/s13054-021-03775-3
46. Cheng YY, Wright CM, Kirschner MB, et al. KCa1.1, a calcium-activated potassium channel subunit alpha 1, is targeted by miR-17-5p and modulates cell migration in malignant pleural mesothelioma. *Mol Cancer*. 2016;15(1):44. doi:10.1186/s12943-016-0529-z
47. Li J, Ye D, Shen P, et al. Mir-20a-5p induced WTX deficiency promotes gastric cancer progressions through regulating PI3K/AKT signaling pathway. *J Exp Clin Cancer Res*. 2020;39(1):212. doi:10.1186/s13046-020-01718-4
48. Liu DL, Lu LL, Dong LL, et al. miR-17-5p and miR-20a-5p suppress postoperative metastasis of hepatocellular carcinoma via blocking HGF/ERBB3-NF-κB positive feedback loop. *Theranostics*. 2020;10(8):3668–3683. doi:10.7150/thno.41365
49. Nguyen HD, Kim MS. Exposure to a mixture of heavy metals induces cognitive impairment: genes and microRNAs involved. *Toxicology*. 2022;471:153164. doi:10.1016/j.tox.2022.153164
50. Kim YM, Krantz S, Jambusaria A, et al. Mitofusin-2 stabilizes adherens junctions and suppresses endothelial inflammation via modulation of β-catenin signaling. *Nat Commun*. 2021;12(1):2736. doi:10.1038/s41467-021-23047-6
51. Luo L, Wei D, Pan Y, et al. MFN2 suppresses clear cell renal cell carcinoma progression by modulating mitochondria-dependent dephosphorylation of EGFR. *Cancer Commun*. 2023;43(7):808–833. doi:10.1002/cac2.12428
52. Li M, Xu B, Li X, et al. Mitofusin 2 confers the suppression of microglial activation by cannabidiol: insights from in vitro and in vivo models. *Brain Behav Immun*. 2022;104:155–170. doi:10.1016/j.bbi.2022.06.003